Real-time Visualization and Analysis of Chondrocyte Injury Due to Mechanical Loading in Fully Intact Murine Cartilage Explants
--Manuscript Draft--

Article Type:	Invited Methods Article - JoVE Produced Video
Manuscript Number:	JoVE58487R1
Full Title:	Real-time Visualization and Analysis of Chondrocyte Injury Due to Mechanical Loading in Fully Intact Murine Cartilage Explants
Keywords:	cell death, chondrocytes, cartilage, mouse model, static loading, impact, trauma
Corresponding Author:	Mark Buckley University of Rochester Rochester, New York UNITED STATES
Corresponding Author's Institution:	University of Rochester
Corresponding Author E-Mail:	mark.buckley@rochester.edu
Order of Authors:	Alexander Kotelsky
	Joseph S Carrier
	Mark Buckley
Additional Information:	
Question	Response
Please indicate whether this article will be Standard Access or Open Access.	Standard Access (US$2,400)
Please indicate the **city, state/province, and country** where this article will be **filmed**. Please do not use abbreviations.	Department of Biomedical Engineering, 321 Robert B. Goergen Hall, University of Rochester, Rochester, NY 14627

Cover Letter

On behalf of my co-authors, please find enclosed our manuscript titled "Real-time Visualization and Analysis of Chondrocyte Death Due to Mechanical Loading in Fully Intact Murine Cartilage Explants" for submission to Journal of Visualized Experiments (JoVE). In this manuscript, we introduce a method that allows for assessment of the spatial extent of cell death induced on the articular surface of mechanically loaded cartilage explants from murine synovial joints. This method requires careful dissections of mouse synovial joints without compromising chondrocyte viability, followed by mechanical testing of vitally stained cartilage explants using a custom microscope-mounted device. Importantly, this method enables testing on fully intact cartilage without compromising native boundary conditions. Moreover, it allows for real-time visualization of vitally stained articular chondrocytes and single image-based analysis of cell injury induced by application of controlled static and impact loading regimens.

Using this method, we have demonstrated that the spatial extent of cell injury depends sensitively on load magnitude and impact intensity. This method can be easily adapted to conduct comparative studies investigating the effects of different controlled environmental and mechanical conditions on the mechanical vulnerability of *in situ* articular chondrocytes. Additionally, the method can be used to screen treatments aimed at reducing the sensitivity of chondrocytes to mechanical stimuli when the tissue is exposed to chronic, abnormal loads (e.g., after a meniscal tear or other joint-destabilizing injury). Consequently, we believe that this manuscript and detailed visualization of the experiments/methods using JoVE's unique multimedia format will be of a great interest to the readers of JoVE, particularly those specializing in cell mechanics, tissue mechanics and murine OA models.

We would also like to confirm that all the listed authors designed the study and helped write the manuscript. Additionally, Alexander Kotelsky and Joseph S. Carrier conducted the experiments.

Senior Science Editor, Nandita Singh, Ph.D., has assisted us in the submission process.

We would like to suggest Lin Han (lh535@drexel.edu, Drexel University), X. Lucas Lu (xlu@udel.edu, University of Delaware), Corinne Henak (chenak@wisc.edu, University of Wisconsin-Madison), Gerard Ateshian (ateshian@columbia.edu, Columbia University), Robert Sah (rsah@ucsd.edu, UC San Diego) and Clark Hung (cth6@columbia.edu, Columbia University) as referees for this manuscript.

Please feel free to contact us if you have any questions.

Sincerely,

Mark. R. Buckley
Department of Biomedical Engineering
201 Robert B. Goergen Hall
Box 270168
University of Rochester
Rochester, NY 14627
Phone: (585) 276-4195
E-mail: mark.buckley@rochester.edu

1   **TITLE:**
2   Real-time Visualization and Analysis of Chondrocyte Injury Due to Mechanical Loading in Fully
3   Intact Murine Cartilage Explants
4
5   **AUTHORS & AFFILIATIONS:**
6   Alexander Kotelsky, Joseph S. Carrier, Mark R. Buckley
7
8   Department of Biomedical Engineering, University of Rochester, Rochester NY, USA
9
10 **EMAIL ADDRESSES:**
11 akotelsk@ur.rochester.edu
12 jcarrie2@u.rochester.edu
13 mark.buckley@rochester.edu
14
15 **CORRESPONDING AUTHOR:**
16 Mark R. Buckley (mark.buckley@rochester.edu)
17
21 **SHORT ABSTRACT:**
22 We present a method to assess the spatial extent of cell injury/death on the articular surface of
23 intact murine joints after application of controlled mechanical loads or impacts. This method can
24 be used to investigate how osteoarthritis, genetic factors and/or different loading regimens
25 affect the vulnerability of *in situ* chondrocytes.
26
27 **LONG ABSTRACT:**
28 Homeostasis of articular cartilage depends on the viability of resident cells (chondrocytes).
29 Unfortunately, mechanical trauma can induce widespread chondrocyte death, potentially
30 leading to irreversible breakdown of the joint and the onset of osteoarthritis. Additionally,
31 maintenance of chondrocyte viability is important in osteochondral graft procedures for optimal
32 surgical outcomes. We present a method to assess the spatial extent of cell injury/death on the
33 articular surface of intact murine synovial joints after application of controlled mechanical loads
34 or impacts. This method can be used in comparative studies to investigate the effects of different
35 mechanical loading regimens, different environmental conditions or genetic manipulations, as
36 well as different stages of cartilage degeneration on short- and/or long-term vulnerability of in
37 situ articular chondrocytes. The goal of the protocol introduced in the manuscript is to assess the
38 spatial extent of cell injury/death on the articular surface of murine synovial joints. Importantly,
39 this method enables testing on fully intact cartilage without compromising native boundary
40 conditions. Moreover, it allows for real-time visualization of vitally stained articular chondrocytes
41 and single image-based analysis of cell injury induced by application of controlled static and
42 impact loading regimens. Our representative results demonstrate that in healthy cartilage
43 explants, the spatial extent of cell injury depends sensitively on load magnitude and impact
44 intensity. Our method can be easily adapted to investigate the effects of different mechanical

45 loading regimens, different environmental conditions or different genetic manipulations on the
46 mechanical vulnerability of *in situ* articular chondrocytes.
47
48 **INTRODUCTION:**
49 Articular cartilage (AC) is a load bearing tissue that covers and protects bones in synovial joints,
50 providing smooth joint articulation. Tissue homeostasis is dependent on the viability of
51 chondrocytes, the sole cell type residing in AC. However, exposure of cartilage to extreme forces
52 due to trauma (*e.g.*, falls, vehicle accident or sports injuries) or due to post-traumatic joint
53 instability can induce chondrocyte death, leading to irreversible breakdown of the joint
54 (osteoarthritis)[1]. Furthermore, in osteochondral grafting procedures that aim to repair local
55 defects in damaged cartilage, graft insertion-associated mechanical trauma reduces chondrocyte
56 viability and has detrimental effects on surgical outcomes[2].
57
58 Cartilage explant models are commonly used to study the susceptibility of articular chondrocytes
59 to mechanically-induced cell death. These models typically use explants from large animals to
60 study the effects of loading conditions, environmental conditions and other factors on cell
61 vulnerability[3-15]. However, due to the large size of the native joints, these models generally
62 require removal of a plug from the articular surface of an intact joint, thereby compromising
63 native boundary conditions. Moreover, they generally require application of large mechanical
64 loads to induce cell injury. Alternatively, murine cartilage explant models provide several
65 advantages over larger animal models in studying the mechanical vulnerability of *in situ*
66 chondrocytes. In particular, due to their smaller dimensions, these models facilitate testing of
67 fully intact articular cartilage without altering native tissue integrity. In addition, loading of
68 murine cartilage occurs over small contact areas such that chondrocyte death/injury can be
69 induced with small loads (<1 N). Finally, the mouse genome is easily manipulated, enabling
70 testing of how specific genes impact the susceptibility of *in situ* chondrocytes to mechanical
71 injury.
72
73 The overall goal of the method introduced in this manuscript is to quantify and visualize—in real-
74 time—the spatial extent of *in situ* cell death/injury due to applied mechanical loads on fully intact
75 mouse cartilage-on-bone explants *in vitro*. This method requires careful dissection of mouse
76 synovial joints without compromising chondrocyte viability, followed by mechanical testing of
77 vitally stained explants using a microscope-mounted device similar to a testing platform that we
78 recently developed to quantify murine cartilage mechanical properties[16]. During mechanical
79 testing, a large portion of the (intact) articular surface of the dissected bone is visible on a single
80 fluorescence micrograph, enabling rapid analysis of cell viability after a load is applied. A similar
81 analysis of surface cell viability in murine cartilage explants has been performed previously, but
82 without simultaneous application of load[17]. Potential applications of our method include
83 comparative studies to investigate the vulnerability of articular chondrocytes to different
84 controlled environmental and mechanical conditions, as well as screening of treatments aimed
85 at reducing the sensitivity of chondrocytes to mechanical loading.
86
87 **PROTOCOL:**
88 All animal work was approved by the University of Rochester Committee on Animal Resources.

89

1. Solutions

1.1) Prepare Hank's Balanced Salt Solution (1X HBSS) containing calcium, magnesium and no phenol red. Adjust the pH to 7.4 by adding small amounts of HCl or NaOH.

1.2) Adjust the osmolarity to 303 mOsm by adding NaCl or deionized water. Use the buffer during the dissections, specimen preparation and mechanical testing.

2. Dissections of the Distal Femur and Proximal Humerus with Fully Intact Articular Cartilage

2.1) Euthanize the mouse according to institutional guidelines using a CO_2 inhalation chamber followed by cervical dislocation. Follow aseptic technique throughout.

NOTE: Mice between 8 and 81 weeks old of any strain and sex may be used.

2.2) Use the following surgical tools for dissections: micro-scissors (used for making incisions), standard dissecting scissors (used for cutting the bone), scalpel with #11 scalpel blade (used for cutting soft tissue), jeweler's forceps (used for removal of soft tissue) and standard forceps (used for peeling the soft tissue and the skin).

2.3) For **dissections of the distal femur** follow the instructions below.

2.3.1) Position the mouse in a supine position.

2.3.2) Make a small (~5 mm) incision in the skin on the anterior portion of the knee.

2.3.3) Extend the incision all the way around the knee and pull back the skin to expose the knee joint and leg muscles.

2.3.4) Starting from the proximal end of the femur, use a scalpel blade (#11) to cut along the distal direction. Position the blade between the quadriceps muscle-tendon unit and the anterior side of the femoral shaft. Extend the cut towards and past the patella and finish by cutting through the middle of the patellar tendon, thereby removing the quadriceps muscle-tendon unit.

2.3.5) Starting from the proximal end of the femur, use a scalpel blade (#11) to cut along the distal direction. Position the blade between the hamstring muscle-tendon unit and the posterior side of the femoral shaft. Once the cut approaches the knee joint, begin cutting through the soft tissue, avoiding contact between the scalpel and the articular surface on the distal condyles of the femur. Finish the cut past the knee joint.

2.3.6) Pull back the quadriceps and hamstring muscles to expose the femur. Cut away any excess muscle on the lateral and medial sides of the femur.

2.3.7) Cut the calf muscle on the posterior side of the proximal tibia and flip the leg to visualize the posterior side of the femur.

2.3.8) Expose the distal condyles of the femur and posterior surface of the proximal tibia by removing excess tissue around the knee joint.

2.3.9) Cut the anterior and posterior cruciate ligaments using a scalpel, cutting away from the femoral condyles. Pull the tibia away from the femur and cut all the ligaments to separate the lower leg from the femur.

2.3.10) Using standard dissecting scissors, cut through the femur at the proximal end of the bone (8 mm above the tibio-femoral joint) from the **lateral** side. After cutting the bone, wipe away any visible marrow on the outside of the bone to avoid possible contamination from bone marrow cells.

NOTE: Cutting from lateral side reduces the risk of crack propagation along the bone.

2.3.11) Remove surrounding soft tissues (*i.e.*, ligaments and excess muscle) from the femur using jeweler's forceps and expose the cartilage on both condyles at the distal end of the femur. Avoid contact between the cartilage and forceps.

2.4) For **dissections of the humerus** follow the instructions below.

2.4.1) Position the mouse in a supine position.

2.4.2) Make an incision (~5 mm) in the skin on the posterior side of the elbow using micro-scissors, extend the incision around the elbow and pull back the skin to expose the muscles of the arm and shoulder.

2.4.3) Starting from the proximal end of the humerus, use a scalpel blade (#11) to cut along the distal direction. Position the blade between the triceps muscle-tendon unit and the posterior side of the humerus. Extend the cut towards the distal end of the humerus and finish by cutting through the triceps tendon.

2.4.4) Then pull back the triceps towards the proximal end of the humerus until the humeral head is exposed.

2.4.5) Cut the connective tissue around the humeral head using a scalpel blade (#11) without touching the articular surface and remove the limb (arm and shoulder) from the body. Periodically hydrate the articular surface of the humeral head with HBSS.

2.4.6) Disconnect the humerus from the arm by first breaking off the proximal end of the ulna on the posterior side of the arm using forceps and then cutting the connective tissue around the distal end of the humerus. Remove any excess tissue on the humerus.

177

2.4.7) Cut off the deltoid tuberosity on the posterior side of the humerus using standard dissecting scissors.

2.5) Place the dissected specimen(s) into a 1.5 mL microcentrifuge tube containing HBSS buffer.

3. Live (Calcein AM) / Dead (Propidium Iodide) Staining Protocol

3.1) Stain using calcein AM as follows.

3.1.1) Make a stock solution of calcein AM by adding 12.5 µL of dimethyl sulfoxide (DMSO) into a vial of 50 µg of calcein AM, resulting in a stock concentration of 4 mg/mL (4.02 mM).

3.1.2) Dilute the stock calcein solution 1:400 in HBSS to reach a concentration of 10 µg/mL (10.05 µM) of calcium AM (for example, add 1.25 µL of stock solution to 500 µL of HBSS).

3.1.3) Centrifuge the diluted staining solution for 5 s at 2000 x g to ensure that all of the dye, which may occasionally stick to the walls of the tube, mixes with the buffer. Do not remove the supernatant. Vortex the solution to ensure proper mixing.

3.1.4) Put the dissected specimen into a 1.5 mL microcentrifuge tube containing 500 µL of the diluted staining solution. Incubate the specimen at 37 °C for 30 min in a thermomixer while agitating at 800 rpm. Make sure the tubes are covered in aluminum foil to protect from exposure to light.

3.1.5) Transfer the specimen into calcein AM-free HBSS buffer. At this point, the specimen is ready for mechanical testing.

3.2) Prepare propidium iodide (PI) staining solution as follows.

3.2.1) Prepare the PI staining solution by diluting the purchased stock solution (1 mg/mL, 1.5 mM) 1:25 in HBSS to reach 40 µg/mL (60 µM) of PI. For example, add 40 µL of stock solution to 1000 µL of HBSS.

3.2.2) Keep the PI staining solution covered in aluminum foil to protect it from exposure to light. Use the staining solution immediate after the mechanical test to detect injured cells (see section 4).

NOTE: One can perform the PI staining prior to loading as well to more rigorously assess the quality of the dissections.

4. Mechanical Testing Protocol

4.1) Place the specimen (femur or humerus) onto the glass slide of a custom microscope-mounted mechanical testing device such that the articular surface on the posterior femoral condyles or humeral head is sitting on the glass (**Figure 1**).

NOTE: Fasten a 10 mm-long wooden applicator (diameter = 2 mm) to the distal side of the **humerus** using cyanoacrylate glue before placing it onto the device in order to stabilize the specimen on the flat surface. For a detailed description of the mechanical testing platform see **Supplementary File 1**: section 1.

4.2) Hydrate the specimen with HBSS and place the device with the specimen onto a fluorescence microscope.

4.3) Image the articular chondrocytes stained with calcein AM (excitation/emission wavelengths = 495/515 nm) before (baseline) application of the load under a fluorescence microscope with a 4X dry lens (NA = 0.13). Adjust the acquisition settings to optimize the image quality.

4.4) Apply mechanical loading on top of the specimen such that articular cartilage is compressed against the cover glass.

4.4.1) For **static loading**, apply a prescribed static load (*e.g.*, 0.5 N) on top of the specimen (femur or humerus). Hold the load for 5 min and then remove it.

4.4.2) For **impact**, apply a prescribed impact energy (*e.g.*, 1 mJ) onto the specimen by dropping a cylindrical impactor of known weight (*e.g.*, 0.1 N) from a prescribed height (*e.g.*, 1 cm). Release the load 5 s after the impact.

NOTE: The weight of the impactor (mg) and the prescribed height (h) can be converted into impact energy (E) using the following equation: E = mgh.

4.5) Incubate the specimen in PI staining solution for 5 min at room temperature.

4.6) Image the articular chondrocytes stained with calcein AM and PI (excitation/emission wavelengths = 535/617 nm) under a fluorescence microscope (**Figure 2**).

5. Data Analysis

5.1) Quantify the area of injured/dead cells due to the applied mechanical loading regimen.

5.1.1) Open the micrographs of the articular surface acquired before and after application of mechanical load in ImageJ[18].

5.1.2) Combine the images into a stack.

5.1.3) Set the scale of the images based on the image resolution.

264
265   5.1.4) Use the **Polygon** tool to define the area where the cells became calcein-negative (loss of
266   green fluorescence) and PI-positive (gain of red fluorescence). These cells are considered to be
267   injured or dead.
268
269   5.1.5) Determine the area of injured/dead cells using the **Measurement** tool.
270
271   **REPRESENTATIVE RESULTS:**
272   Six different applied loading protocols (static loading: 0.1 N, 0.5 N and 1 N for 5 min; and impact
273   loading: 1 mJ, 2 mJ and 4 mJ) reproducibly induced quantifiable localized areas of cell injury in
274   femoral and humeral cartilage obtained from 8-10-week-old BALB/c mice (**Figure 2**). Importantly,
275   the spatial extent of chondrocyte injury on the articular surface was measured quickly and easily
276   in ImageJ. Representative results demonstrate that the mechanical vulnerability of articular
277   chondrocytes was affected by load magnitude and impact intensity. In particular, higher load
278   magnitudes and higher impact intensities significantly exacerbated the spatial extent of cell injury
279   in both femurs and humeri (**Figure 3**).
280
281   **FIGURE LEGENDS:**
282
283   **Figure 1: Schematic representation of the custom mechanical testing device.** (**a**) Assembled
284   device with the cylindrical impactor used to apply prescribed mechanical loads and/or impact
285   energies to a specimen. The device is shown without a specimen. (**b**) Schematic representation
286   of the experiment. Controlled static (*e.g.*, 0.1 N) and/or impact (*e.g.*, 1 mJ) loading can be applied
287   on top of the dissected specimen such that articular cartilage is compressed against the cover
288   glass.
289
290   **Figure 2: Representative micrograph of the articular surface after injurious mechanical loading.**
291   Representative micrograph of the articular surface on (**a**) the distal femoral condyles and (**b**) the
292   humeral head after injurious mechanical loading (impact [1 mJ] and static loading [1 N],
293   respectively). Green cells are vitally stained chondrocytes with intact cell membranes while red
294   nuclei indicate injured cells with permeabilized cell membranes. (**c**) Zoomed-in view of the area
295   of injured/dead cells (yellow contours) on the articular surface of the humeral head.
296
297   **Figure 3: Area of injured/dead cells.** Area of injured/dead cells on the articular surface of the
298   distal femoral condyles (**a**, **b**) and the humeral head (**c**, **d**) after (**a**, **c**) static (0.1 N, 0.5 N and 1 N;
299   n = 6 per group) and (**b**, **d**) impact (1 mJ, 2 mJ and 4 mJ; n = 6 per group) loading. All cartilage-on-
300   bone specimens were obtained from female BALB/c 8-10 weeks old mice. Data are mean +
301   standard deviation; brackets denote statistical significance at $\alpha=0.05$ determined by analysis of
302   variance (ANOVA) test with Tukey *post hoc* comparisons.
303
304   **DISCUSSION:**
305   The methods described above were successfully employed to visualize viable and injured/dead
306   *in situ* articular chondrocytes from mouse joints after prescribed mechanical loads or impacts. In
307   particular, we were able to analyze the mechanical vulnerability of chondrocytes within fully

308 intact articular cartilage from two different synovial joints: the knee joint (distal femurs) and
309 shoulder (humeri). Our representative results show that the spatial extent of cell injury on the
310 articular surface depends sensitively on load magnitude and impact intensity (**Figure 3**).
311 Importantly, the use of this method facilitates investigations of the cellular response to
312 mechanical loading under physiologically relevant conditions. That is, it enables testing of
313 articular cartilage on an **intact** joint under physiological and supraphysiological loads (see
314 **Supplementary File 1**: section 2).

316 Given the steep learning curve in performing dissections of murine synovial joints and challenges
317 in preserving viable *in situ* chondrocytes at baseline, some protocol modification and
318 troubleshooting may be required. The greatest risk of damaging articular chondrocytes during
319 dissection occurs during steps 2.3.5 through 2.3.10 and 2.4.5 through 2.4.7. To minimize cell
320 injury/death during dissections, the researcher should avoid any contact between surgical tools
321 (*e.g.*, the scalpel when cutting the tissue or the jeweler's forceps when removing the soft tissue)
322 and the articular surface of the specimen. However, touching the articular surface with a glove
323 induces little cell injury/death. In order to improve baseline cell viability, it may also be necessary
324 to reduce the amount of soft tissue removed from the joint. Additionally, using finer tools will
325 generally reduce dissection-induced cell death. Ultimately, to rigorously confirm the absence of
326 dissection-associated damage of articular chondrocytes at baseline, it is advisable to stain the
327 specimens with both permeability dyes (calcein AM and PI, prior to loading) especially while the
328 researcher is becoming familiar with the dissection procedure (see **Supplemental File 1**: section
329 3).

331 Given the small size of the mouse joint and the genetic manipulability of the mouse genome,
332 murine models provide multiple advantages over large animal models to study vulnerability of
333 articular chondrocytes to mechanical loading. However, to the authors' knowledge, no studies
334 have previously been conducted to quantify injury/death of *in situ* articular chondrocytes due to
335 mechanical loading of intact murine cartilage. Investigators typically use explants removed from
336 joints of large animal models to investigate the extent of cell death due to mechanical injury[3-12].
337 In contrast, mouse models facilitate 1) visualization of nearly the entire articular surface on a
338 given bone; and 2) analyses of post-loading or post-impact chondrocyte viability in intact joints
339 without compromising native boundary conditions. Furthermore, while compressed, mouse
340 specimens generate substantially smaller contact areas compared to large animal models;
341 therefore, stresses are dramatically higher than in large animal models for a given load
342 magnitude. Hence, cell injury can be induced by smaller loads. Additionally, murine models
343 facilitate research on cartilage degeneration and, in particular, osteoarthritis, as this disease can
344 be easily induced in mice through genetic[19-22], dietary[23,24] or surgical manipulations[25-28].
345 Moreover, spontaneous osteoarthritis occurs in several mouse strains including BALB/c and
346 C57BL/6[29,30].

348 In our representative data, we used viability (live/dead) stains to quantify cell injury/death 5 min
349 after the removal of mechanical loading. We acknowledge that these experiments may not
350 discriminate injured cells (cells with temporarily ruptured membranes) from dead cells (cells with
351 permanently ruptures membranes). That is, cells that are calcein negative and PI positive—

352 indicating that the membrane was previously permeabilized—may repair their membranes over
353 time scales ranging from seconds to several minutes[31]. In fact, in a separate set of experiments,
354 we have determined that the fraction of "injured" cells that survive mechanical trauma is small
355 (~5%) but significant (see **Supplementary File 1**: section 4). Therefore, live/dead staining is a
356 direct measure of membrane integrity that is not always indicative of cell viability. In particular,
357 PI-positive and calcein-negative cells are most appropriately defined as "injured", where injury is
358 defined as a (potentially temporary) loss of plasma membrane integrity due to mechanical
359 trauma. We also acknowledge that our representative data likely reflects only immediate
360 (necrotic) cell death. Imaging specimens at later time points (*e.g.*, 48 h after removal of load)
361 should enable quantification of both necrotic and apoptotic cell death.

363 Several limitations must be considered when using these methods. In our trial experiments for
364 this manuscript, we used 8-10-weeks-old female BALB/c mice to demonstrate the capabilities of
365 the testing platform (**Figure 3**). However, due to noticeable alterations in cell density in femurs
366 of older mice, the assessment of load-induced cell injury becomes more challenging (though
367 feasible) in older femurs (success rate = 40%). In contrast, no noticeable alterations in cell density
368 on humeri were observed in 61-81-week-old C57BL/6 mice (see **Supplementary File 1**: section
369 5), thereby making the testing platform useful for ages 8-81 weeks. Another limitation is that the
370 method was used to analyze the spatial extent of cell injury only on the articular surface of
371 femoral condyles and humeral head. However, the method could further be extended to analyze
372 depth-dependent spatial extent of cell injury through use of laser scanning confocal microscopy.
373 Note that the latter method would require usage of more expensive equipment, longer image
374 acquisition time, and more involved and time-consuming analysis. Finally, although the contact
375 location between the articular cartilage and the cover glass was physiologically relevant for
376 mice[32,33], this location was not varied. However, our testing platform allows for variation of the
377 contact location if the femur or humerus is gripped with a rotating armature.

379 In conclusion, we have developed an *in vitro* murine injury model that enables application of
380 controlled mechanical loads and/or impacts onto the articular surface of intact articular cartilage.
381 This model enables visualization of fluorescently labeled articular chondrocytes in real-time and
382 rapid single image-based analysis of cell injury/death. Importantly, the effects of different
383 mechanical loading regimens, different environmental conditions or different genetic
384 manipulations on short- and/or long-term chondrocyte viability can be tested using this
385 methodology. Thus, our platform provides a tool to interrogate basic science questions and
386 screen therapeutic targets related to the mechanical vulnerability of chondrocytes.

394 **DISCLOSURES:**
395 The authors have nothing to disclose.

REFERENCES:

1   Lotz, M. K. & Kraus, V. B. New developments in osteoarthritis. Posttraumatic osteoarthritis: pathogenesis and pharmacological treatment options. *Arthritis Research & Therapy.* **12** (3), 211, doi:10.1186/ar3046, (2010).

2   Pallante, A. L. *et al.* The *in vivo* performance of osteochondral allografts in the goat is diminished with extended storage and decreased cartilage cellularity. *American Journal of Sports Medicine.* **40** (8), 1814-1823, doi:10.1177/0363546512449321, (2012).

3   Delco, M. L., Bonnevie, E. D., Bonassar, L. J. & Fortier, L. A. Mitochondrial dysfunction is an acute response of articular chondrocytes to mechanical injury. *Journal of Orthopaedic Research.* **36** (2), 739-750, doi:10.1002/jor.23651, (2018).

4   Ewers, B. J., Dvoracek-Driksna, D., Orth, M. W. & Haut, R. C. The extent of matrix damage and chondrocyte death in mechanically traumatized articular cartilage explants depends on rate of loading. *Journal of Orthopaedic Research.* **19** (5), 779-784, doi:10.1016/S0736-0266(01)00006-7, (2001).

5   Goodwin, W. *et al.* Rotenone prevents impact-induced chondrocyte death. *Journal of Orthopaedic Research.* **28** (8), 1057-1063, doi:10.1002/jor.21091, (2010).

6   Issa, R., Boeving, M., Kinter, M. & Griffin, T. M. Effect of biomechanical stress on endogenous antioxidant networks in bovine articular cartilage. *Journal of Orthopaedic Research.* **36** (2), 760-769, doi:10.1002/jor.23728, (2018).

7   Bartell, L. R., Fortier, L. A., Bonassar, L. J. & Cohen, I. Measuring microscale strain fields in articular cartilage during rapid impact reveals thresholds for chondrocyte death and a protective role for the superficial layer. *Journal of Biomechanics.* **48** (12), 3440-3446, doi:10.1016/j.jbiomech.2015.05.035, (2015).

8   Levin, A. S., Chen, C. T. & Torzilli, P. A. Effect of tissue maturity on cell viability in load-injured articular cartilage explants. *Osteoarthritis and Cartilage.* **13** (6), 488-496, doi:10.1016/j.joca.2005.01.006, (2005).

9   Lee, W. *et al.* Synergy between Piezo1 and Piezo2 channels confers high-strain mechanosensitivity to articular cartilage. *Proceedings of the National Academy of Sciences of the United States of America.* **111** (47), E5114-5122, doi:10.1073/pnas.1414298111, (2014).

10   Jeffrey, J. E., Gregory, D. W. & Aspden, R. M. Matrix damage and chondrocyte viability following a single impact load on articular cartilage. *Archives of Biochemistry and Biophysics.* **322** (1), 87-96, doi:10.1006/abbi.1995.1439, (1995).

11   Chen, C. T., Bhargava, M., Lin, P. M. & Torzilli, P. A. Time, stress, and location dependent chondrocyte death and collagen damage in cyclically loaded articular cartilage. *Journal of Orthopaedic Research.* **21** (5), 888-898, doi:10.1016/S0736-0266(03)00050-0, (2003).

12   Morel, V., Mercay, A. & Quinn, T. M. Prestrain decreases cartilage susceptibility to injury by ramp compression *in vitro*. *Osteoarthritis and Cartilage.* **13** (11), 964-970, doi:10.1016/j.joca.2005.06.016, (2005).

13   Sauter, E., Buckwalter, J. A., McKinley, T. O. & Martin, J. A. Cytoskeletal dissolution blocks oxidant release and cell death in injured cartilage. *Journal of Orthopaedic Research.* **30** (4), 593-598, doi:10.1002/jor.21552, (2012).

14   Martin, J. A. & Buckwalter, J. A. Post-traumatic osteoarthritis: the role of stress induced chondrocyte damage. *Biorheology.* **43** (3,4), 517-521 (2006).

440   15   Martin, J. A., Brown, T., Heiner, A. & Buckwalter, J. A. Post-traumatic osteoarthritis: the
441   role of accelerated chondrocyte senescence. *Biorheology.* **41** (3-4), 479-491 (2004).
442   16   Kotelsky, A., Woo, C. W., Delgadillo, L. F., Richards, M. S. & Buckley, M. R. An Alternative
443   Method to Characterize the Quasi-Static, Nonlinear Material Properties of Murine Articular
444   Cartilage. *Journal of Biomechanical Engineering.* **140** (1), doi:10.1115/1.4038147, (2018).
445   17   Zhang, M. *et al.* Induced superficial chondrocyte death reduces catabolic cartilage
446   damage in murine posttraumatic osteoarthritis. *Journal of Clinical Investigation.* **126** (8), 2893-
447   2902, doi:10.1172/JCI83676, (2016).
448   18   Schneider, C. A., Rasband, W. S. & Eliceiri, K. W. NIH Image to ImageJ: 25 years of image
449   analysis. *Nature Methods.* **9** (7), 671-675 (2012).
450   19   Habouri, L. *et al.* Deletion of 12/15-lipoxygenase accelerates the development of aging-
451   associated and instability-induced osteoarthritis. *Osteoarthritis and Cartilage.* **25** (10), 1719-
452   1728, doi:10.1016/j.joca.2017.07.001, (2017).
453   20   Higuchi, Y. *et al.* Conditional knockdown of hyaluronidase 2 in articular cartilage
454   stimulates osteoarthritic progression in a mice model. *Scientific Reports.* **7** (1), 7028,
455   doi:10.1038/s41598-017-07376-5, (2017).
456   21   Zhu, M. *et al.* Activation of beta-catenin signaling in articular chondrocytes leads to
457   osteoarthritis-like phenotype in adult beta-catenin conditional activation mice. *Journal of Bone
458   and Mineral Research.* **24** (1), 12-21, doi:10.1359/jbmr.080901, (2009).
459   22   Hu, K. *et al.* Pathogenesis of osteoarthritis-like changes in the joints of mice deficient in
460   type IX collagen. *Arthritis & Rheumatology.* **54** (9), 2891-2900, doi:10.1002/art.22040, (2006).
461   23   Mooney, R. A., Sampson, E. R., Lerea, J., Rosier, R. N. & Zuscik, M. J. High-fat diet
462   accelerates progression of osteoarthritis after meniscal/Ligamentous injury. *Arthritis Research &
463   Therapy.* **13** (6), R198, doi:10.1186/ar3529, (2011).
464   24   Griffin, T. M., Huebner, J. L., Kraus, V. B., Yan, Z. & Guilak, F. Induction of osteoarthritis
465   and metabolic inflammation by a very high-fat diet in mice: effects of short-term exercise.
466   *Arthritis & Rheumatology.* **64** (2), 443-453, doi:10.1002/art.33332, (2012).
467   25   Kamekura, S. *et al.* Osteoarthritis development in novel experimental mouse models
468   induced by knee joint instability. *Osteoarthritis and Cartilage.* **13** (7), 632-641,
469   doi:10.1016/j.joca.2005.03.004, (2005).
470   26   Glasson, S. S., Blanchet, T. J. & Morris, E. A. The surgical destabilization of the medial
471   meniscus (DMM) model of osteoarthritis in the 129/SvEv mouse. *Osteoarthritis and Cartilage.* **15**
472   (9), 1061-1069, doi:10.1016/j.joca.2007.03.006, (2007).
473   27   Huang, H., Skelly, J. D., Ayers, D. C. & Song, J. Age-dependent Changes in the Articular
474   Cartilage and Subchondral Bone of C57BL/6 Mice after Surgical Destabilization of Medial
475   Meniscus. *Scientific Reports.* **7** 42294, doi:10.1038/srep42294, (2017).
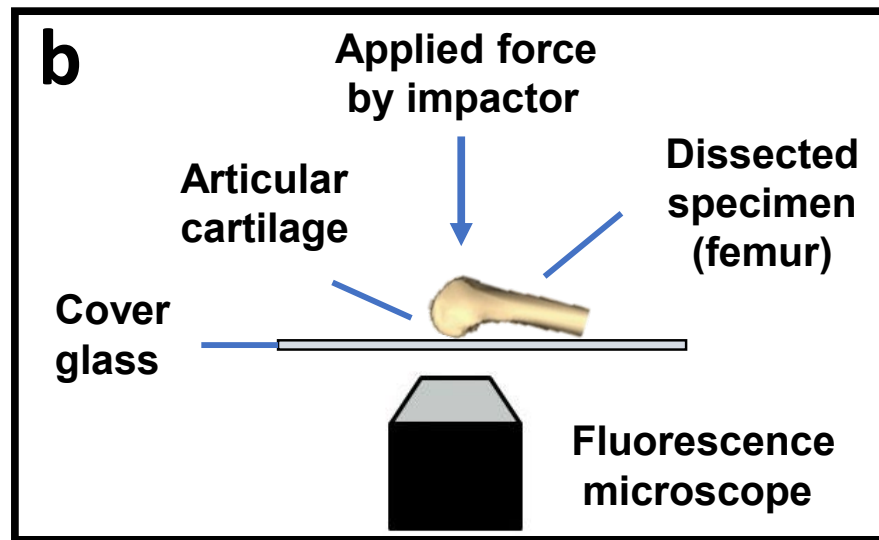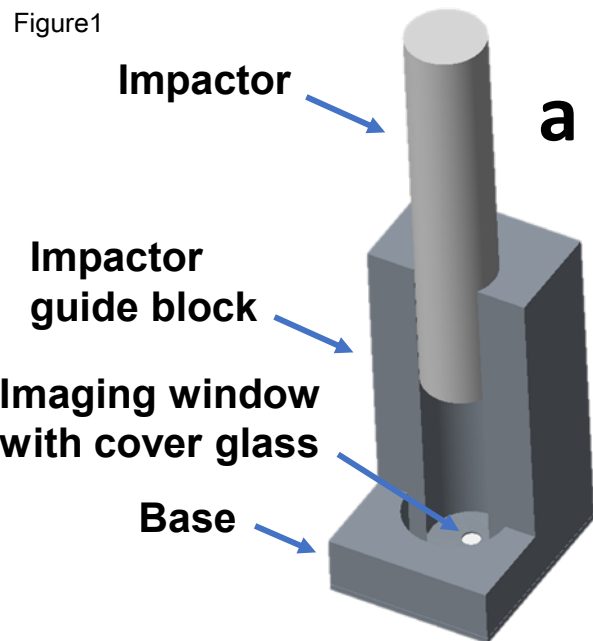476   28   Hamada, D., Sampson, E. R., Maynard, R. D. & Zuscik, M. J. Surgical induction of
477   posttraumatic osteoarthritis in the mouse. *Methods in Molecular Biology.* **1130** 61-72,
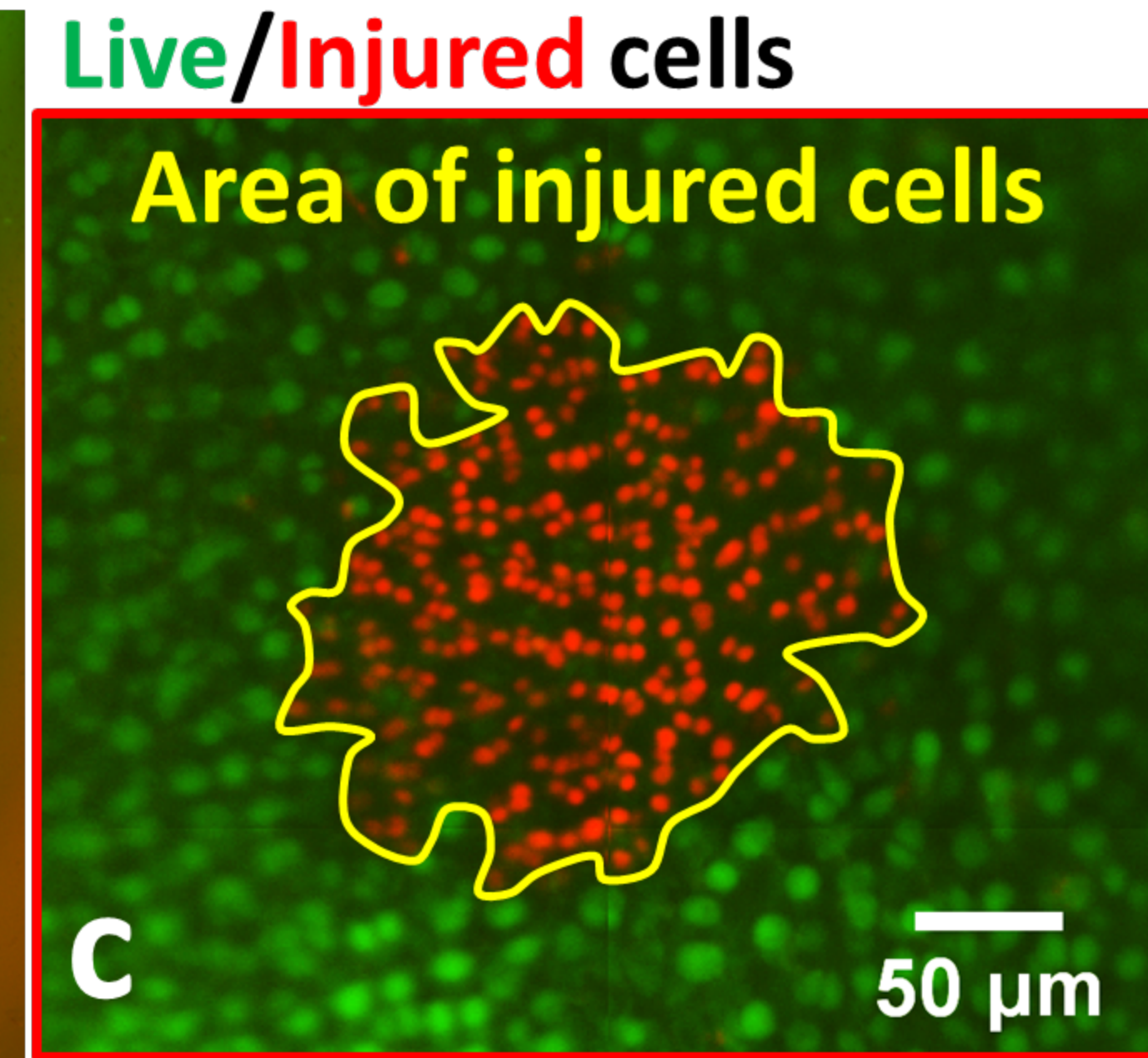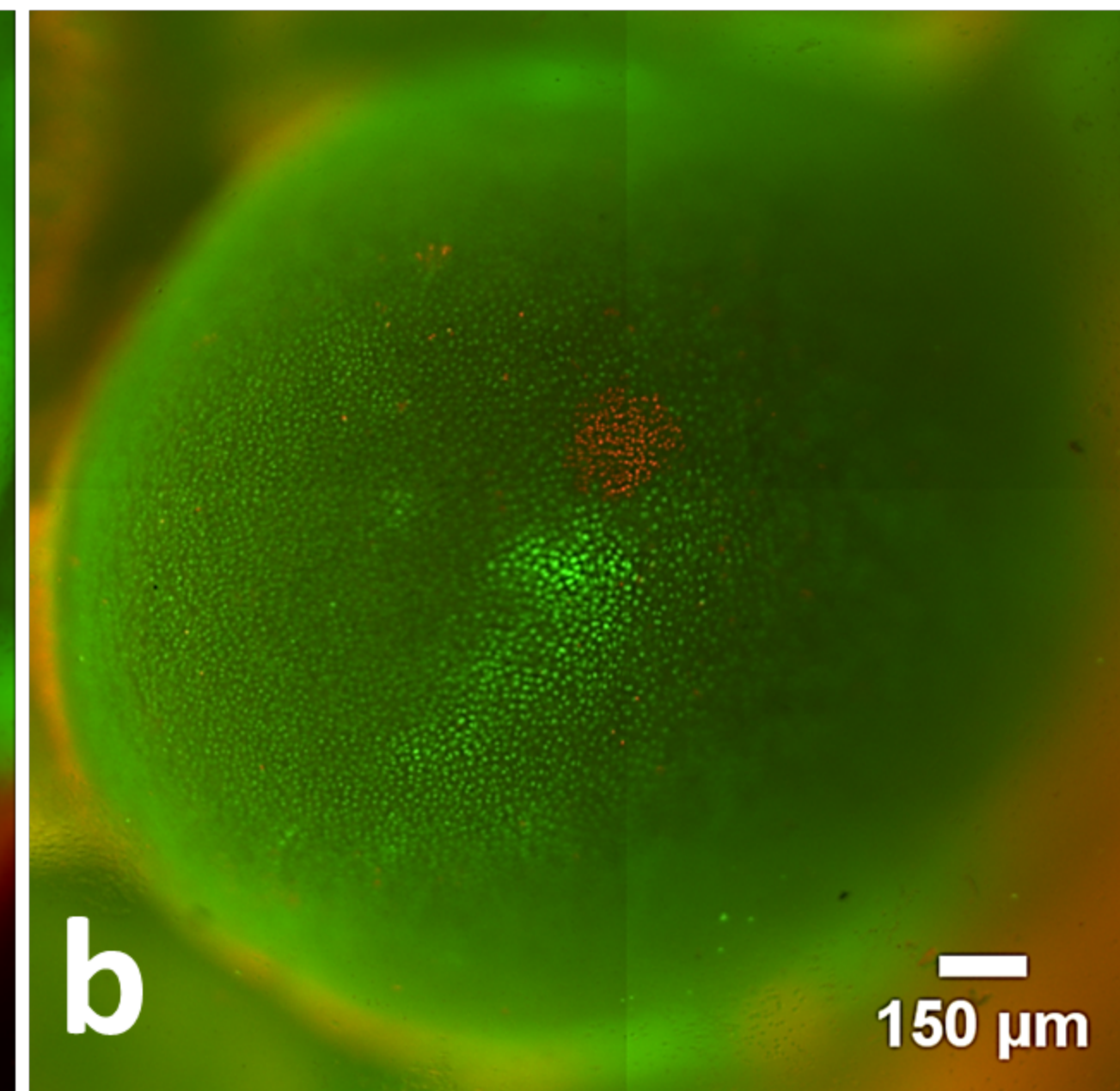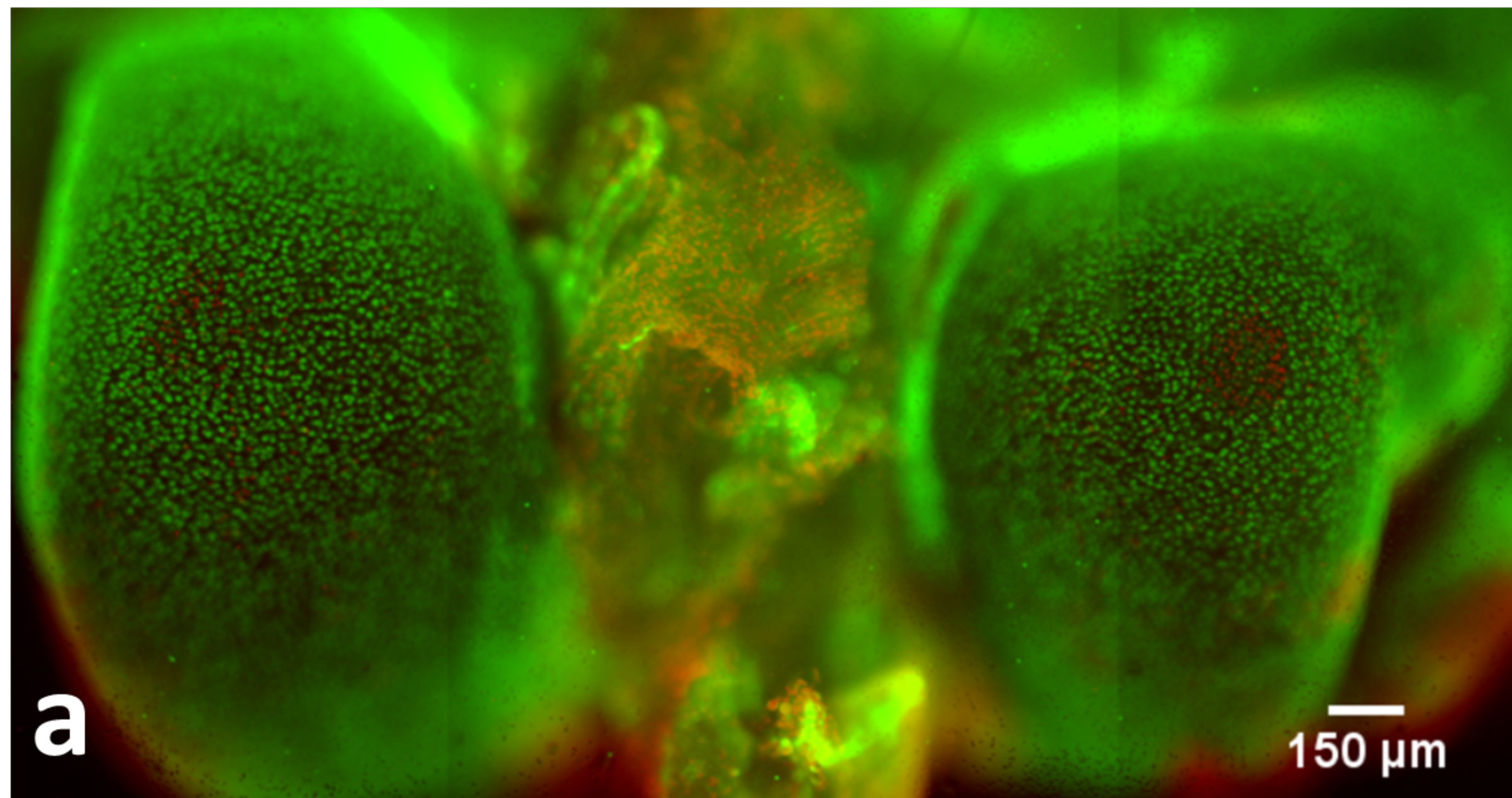478   doi:10.1007/978-1-62703-989-5_5, (2014).
479   29   Wilhelmi, G. & Faust, R. Suitability of the C57 black mouse as an experimental animal for
480   the study of skeletal changes due to ageing, with special reference to osteo-arthrosis and its
481   response to tribenoside. *Pharmacology.* **14** (4), 289-296, doi:10.1159/000136607, (1976).
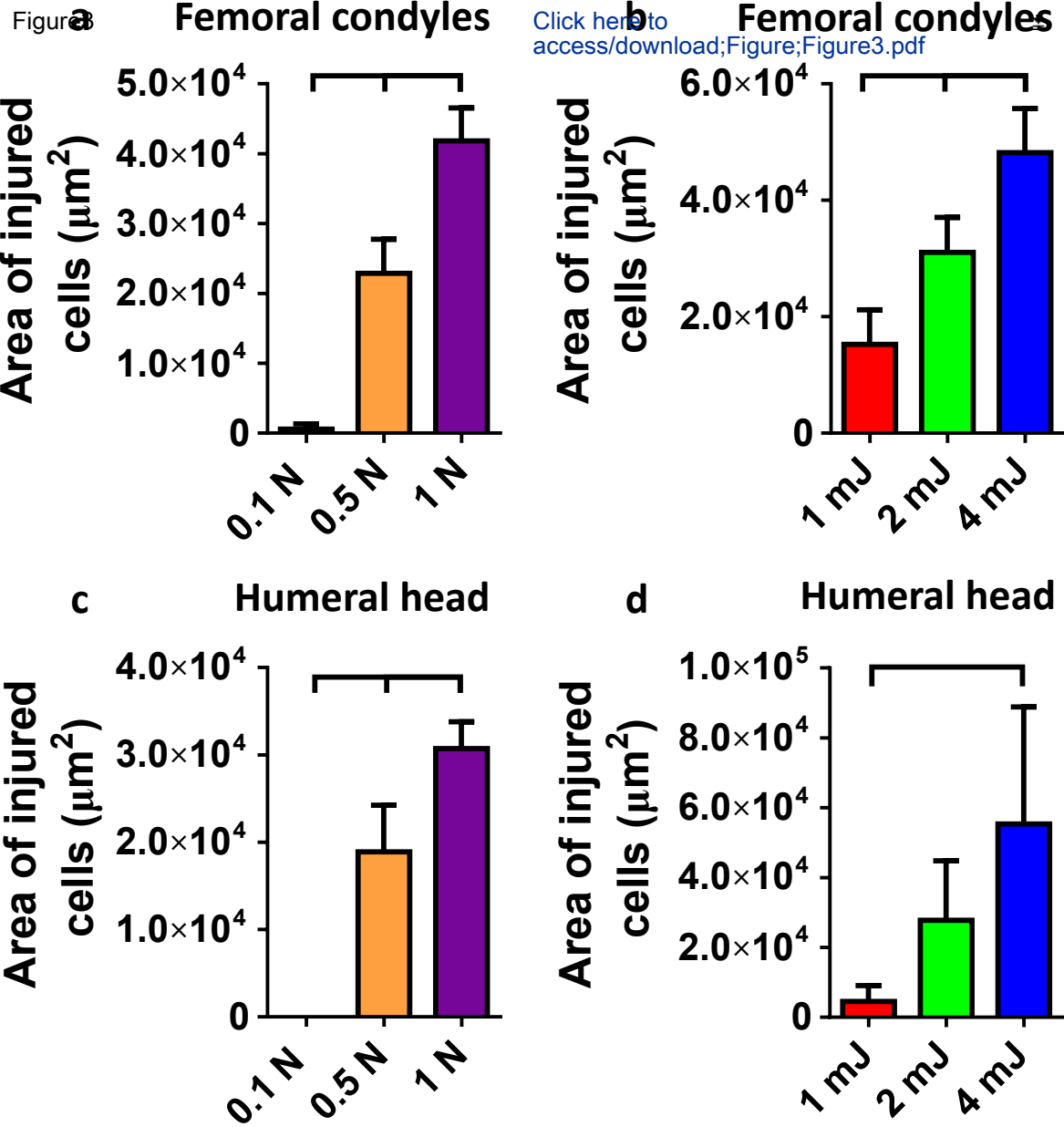
482   30   Stoop, R. *et al.* Type II collagen degradation in spontaneous osteoarthritis in C57Bl/6 and
483   BALB/c mice. *Arthritis & Rheumatism.* **42** (11), 2381-2389, doi:10.1002/1529-
484   0131(199911)42:11<2381::AID-ANR17>3.0.CO;2-E, (1999).
485   31   McNeil, P. L. & Kirchhausen, T. An emergency response team for membrane repair.
486   *Nature Reviews Molecular Cell Biology.* **6** (6), 499-505, doi:10.1038/nrm1665, (2005).
487   32   Adebayo, O. O. *et al.* Kinematics of meniscal- and ACL-transected mouse knees during
488   controlled tibial compressive loading captured using roentgen stereophotogrammetry. *Journal*
489   *of Orthopaedic Research.* **35** (2), 353-360, doi:10.1002/jor.23285, (2017).
490   33   Vahedipour, A. *et al.* Uncovering the structure of the mouse gait controller: Mice respond
491   to substrate perturbations with adaptations in gait on a continuum between trot and bound.
492   *Journal of Biomechanics.* doi:10.1016/j.jbiomech.2018.07.020, (2018).
493

Figure1

a
Impactor
Impactor guide block
Imaging window with cover glass
Base

b
Applied force by impactor
Articular cartilage
Dissected specimen (femur)
Cover glass
Fluorescence microscope

Figure2

Click here to access/download;Figure;Figure2.pdf ⬆

Live/Injured cells

Area of injured cells

a

b

c

150 µm

150 µm

50 µm

Figure 3

a Femoral condyles

b Femoral condyles

c Humeral head

d Humeral head

Materials Table

Click here to access/download;Table of Materials;JoVE_Materials.xlsx ⬇

Name of Reagent/ Equipment	Company	Catalog Number
Calcein, AM	Invitrogen by Thermo Fisher Scientific	C3100MP
Propidium Iodide	Invitrogen by Thermo Fisher Scientific	P3566
Dimethyl sulfoxide (DMSO)	Sigma-Aldrich	276855
HBSS (calcium, magnesium, no phenol red)	Gibco by Thermo Fisher Scientific	14025-092
Feather surgical blade (#11)	VWR	102097-822
Vapor pressure osmometer, VAPRO	ELITechGroup	Model 5520
pH meter	Beckman	Model Phi 32
Eppendorf thermomixer	Eppendorf AG	Model 5350
Motorized inverted research microscope	Olypmus	Model IX-81
Wooden applicator	Puritan Medical Products Company, LLC	807
1.5 Glass coverslips	Warner Instruments, LLC	64-1696

Comments/Description

20x50μg , Eugene, OR, USA

1 mg/mL solution in water, 10mL, Eugene, OR, USA

1L DMSO, anhydrous, ≥99.9%, St. Louis, MO, USA

1X, 500mL, Grand Island, NY, USA

Hatfield, PA, USA

Puteaux, France

Brea, CA, USA
Hamburg, Germany

Center Valley, PA, USA

6"x100, Guilford, ME, USA

#1.5, 0.17mm thick, 40mm diameter, Hamden, CT, USA

jove
JOURNAL OF
VISUALIZED EXPERIMENTS

1 Alewife Center #200
Cambridge, MA 02140
tel. 617.945.9051
www.jove.com

ARTICLE AND VIDEO LICENSE AGREEMENT

Title of Article:

Real-time Visualization and Analysis of Chondrocyte Death Due to Mechanical Loading in Fully Intact Murine Cartilage Explants

Author(s):

Alexander Kotelsky, Joseph S. Carrier, Mark R. Buckley

Item 1 (check one box): The Author elects to have the Materials be made available (as described at http://www.jove.com/author) via: **[X]** Standard Access   [ ] Open Access

Item 2 (check one box):

[X] The Author is NOT a United States government employee.

[ ] The Author is a United States government employee and the Materials were prepared in the course of his or her duties as a United States government employee.

[ ] The Author is a United States government employee but the Materials were NOT prepared in the course of his or her duties as a United States government employee.

ARTICLE AND VIDEO LICENSE AGREEMENT

1. <u>Defined Terms</u>. As used in this Article and Video License Agreement, the following terms shall have the following meanings: "**Agreement**" means this Article and Video License Agreement; "**Article**" means the article specified on the last page of this Agreement, including any associated materials such as texts, figures, tables, artwork, abstracts, or summaries contained therein; "**Author**" means the author who is a signatory to this Agreement; "**Collective Work**" means a work, such as a periodical issue, anthology or encyclopedia, in which the Materials in their entirety in unmodified form, along with a number of other contributions, constituting separate and independent works in themselves, are assembled into a collective whole; "**CRC License**" means the Creative Commons Attribution-Non Commercial-No Derivs 3.0 Unported Agreement, the terms and conditions of which can be found at: http://creativecommons.org/licenses/by-nc-nd/3.0/legalcode; "**Derivative Work**" means a work based upon the Materials or upon the Materials and other pre-existing works, such as a translation, musical arrangement, dramatization, fictionalization, motion picture version, sound recording, art reproduction, abridgment, condensation, or any other form in which the Materials may be recast, transformed, or adapted; "**Institution**" means the institution, listed on the last page of this Agreement, by which the Author was employed at the time of the creation of the Materials; "**JoVE**" means MyJove Corporation, a Massachusetts corporation and the publisher of *The Journal of Visualized Experiments*; "**Materials**" means the Article and / or the Video; "**Parties**" means the Author and JoVE; "**Video**" means any video(s) made by the Author, alone or in conjunction with any other parties, or by JoVE or its affiliates or agents, individually or in collaboration with the Author or any other parties, incorporating all or any portion of the Article, and in which the Author may or may not appear.

2. <u>Background</u>. The Author, who is the author of the Article, in order to ensure the dissemination and protection of the Article, desires to have the JoVE publish the Article and create and transmit videos based on the Article. In furtherance of such goals, the Parties desire to memorialize in this Agreement the respective rights of each Party in and to the Article and the Video.

3. <u>Grant of Rights in Article</u>. In consideration of JoVE agreeing to publish the Article, the Author hereby grants to JoVE, subject to **Sections 4 and 7** below, the exclusive, royalty-free, perpetual (for the full term of copyright in the Article, including any extensions thereto) license (a) to publish, reproduce, distribute, display and store the Article in all forms, formats and media whether now known or hereafter developed (including without limitation in print, digital and electronic form) throughout the world, (b) to translate the Article into other languages, create adaptations, summaries or extracts of the Article or other Derivative Works (including, without limitation, the Video) or Collective Works based on all or any portion of the Article and exercise all of the rights set forth in (a) above in such translations, adaptations, summaries, extracts, Derivative Works or Collective Works and (c) to license others to do any or all of the above. The foregoing rights may be exercised in all media and formats, whether now known or hereafter devised, and include the right to make such modifications as are technically necessary to exercise the rights in other media and formats. If the "Open Access" box has been checked in **Item 1** above, JoVE and the Author hereby grant to the public all such rights in the Article as provided in, but subject to all limitations and requirements set forth in, the CRC License.

1

612542 6

4. Retention of Rights in Article. Notwithstanding the exclusive license granted to JoVE in Section 3 above, the Author shall, with respect to the Article, retain the non-exclusive right to use all or part of the Article for the non-commercial purpose of giving lectures, presentations or teaching classes, and to post a copy of the Article on the Institution's website or the Author's personal website, in each case provided that a link to the Article on the JoVE website is provided and notice of JoVE's copyright in the Article is included. All non-copyright intellectual property rights in and to the Article, such as patent rights, shall remain with the Author.

5. Grant of Rights in Video – Standard Access. This Section 5 applies if the "Standard Access" box has been checked in Item 1 above or if no box has been checked in Item 1 above. In consideration of JoVE agreeing to produce, display or otherwise assist with the Video, the Author hereby acknowledges and agrees that, Subject to Section 7 below, JoVE is and shall be the sole and exclusive owner of all rights of any nature, including, without limitation, all copyrights, in and to the Video. To the extent that, by law, the Author is deemed, now or at any time in the future, to have any rights of any nature in or to the Video, the Author hereby disclaims all such rights and transfers all such rights to JoVE.

6. Grant of Rights in Video – Open Access. This Section 6 applies only if the "Open Access" box has been checked in Item 1 above. In consideration of JoVE agreeing to produce, display or otherwise assist with the Video, the Author hereby grants to JoVE, subject to Section 7 below, the exclusive, royalty-free, perpetual (for the full term of copyright in the Article, including any extensions thereto) license (a) to publish, reproduce, distribute, display and store the Video in all forms, formats and media whether now known or hereafter developed (including without limitation in print, digital and electronic form) throughout the world, (b) to translate the Video into other languages, create adaptations, summaries or extracts of the Video or other Derivative Works or Collective Works based on all or any portion of the Video and exercise all of the rights set forth in (a) above in such translations, adaptations, summaries, extracts, Derivative Works or Collective Works and (c) to license others to do any or all of the above. The foregoing rights may be exercised in all media and formats, whether now known or hereafter devised, and include the right to make such modifications as are technically necessary to exercise the rights in other media and formats. For any Video to which this Section 6 is applicable, JoVE and the Author hereby grant to the public all such rights in the Video as provided in, but subject to all limitations and requirements set forth in, the CRC License.

7. Government Employees. If the Author is a United States government employee and the Article was prepared in the course of his or her duties as a United States government employee, as indicated in Item 2 above, and any of the licenses or grants granted by the Author hereunder exceed the scope of the 17 U.S.C. 403, then the rights granted hereunder shall be limited to the maximum rights permitted under such statute. In such case, all provisions contained herein that are not in conflict with such statute shall remain in full force and effect, and all provisions contained herein that do so conflict shall be deemed to be amended so as to provide to JoVE the maximum rights permissible within such statute.

8. Likeness, Privacy, Personality. The Author hereby grants JoVE the right to use the Author's name, voice, likeness, picture, photograph, image, biography and performance in any way, commercial or otherwise, in connection with the Materials and the sale, promotion and distribution thereof. The Author hereby waives any and all rights he or she may have, relating to his or her appearance in the Video or otherwise relating to the Materials, under all applicable privacy, likeness, personality or similar laws.

9. Author Warranties. The Author represents and warrants that the Article is original, that it has not been published, that the copyright interest is owned by the Author (or, if more than one author is listed at the beginning of this Agreement, by such authors collectively) and has not been assigned, licensed, or otherwise transferred to any other party. The Author represents and warrants that the author(s) listed at the top of this Agreement are the only authors of the Materials. If more than one author is listed at the top of this Agreement and if any such author has not entered into a separate Article and Video License Agreement with JoVE relating to the Materials, the Author represents and warrants that the Author has been authorized by each of the other such authors to execute this Agreement on his or her behalf and to bind him or her with respect to the terms of this Agreement as if each of them had been a party hereto as an Author. The Author warrants that the use, reproduction, distribution, public or private performance or display, and/or modification of all or any portion of the Materials does not and will not violate, infringe and/or misappropriate the patent, trademark, intellectual property or other rights of any third party. The Author represents and warrants that it has and will continue to comply with all government, institutional and other regulations, including, without limitation all institutional, laboratory, hospital, ethical, human and animal treatment, privacy, and all other rules, regulations, laws, procedures or guidelines, applicable to the Materials, and that all research involving human and animal subjects has been approved by the Author's relevant institutional review board.

10. JoVE Discretion. If the Author requests the assistance of JoVE in producing the Video in the Author's facility, the Author shall ensure that the presence of JoVE employees, agents or independent contractors is in accordance with the relevant regulations of the Author's institution. If more than one author is listed at the beginning of this Agreement, JoVE may, in its sole discretion, elect not take any action with respect to the Article until such time as it has received complete, executed Article and Video License Agreements from each such author. JoVE reserves the right, in its absolute and sole discretion and without giving any reason therefore, to accept or decline any work submitted to JoVE. JoVE and its employees, agents and independent contractors shall have

2

ARTICLE AND VIDEO LICENSE AGREEMENT

jove
JOURNAL OF
VISUALIZED EXPERIMENTS

1 Alewife Center #200
Cambridge, MA 02140
tel. 617.945.9051
www.jove.com

full, unfettered access to the facilities of the Author or of the Author's institution as necessary to make the Video, whether actually published or not. JoVE has sole discretion as to the method of making and publishing the Materials, including, without limitation, to all decisions regarding editing, lighting, filming, timing of publication, if any, length, quality, content and the like.

11. Indemnification. The Author agrees to indemnify JoVE and/or its successors and assigns from and against any and all claims, costs, and expenses, including attorney's fees, arising out of any breach of any warranty or other representations contained herein. The Author further agrees to indemnify and hold harmless JoVE from and against any and all claims, costs, and expenses, including attorney's fees, resulting from the breach by the Author of any representation or warranty contained herein or from allegations or instances of violation of intellectual property rights, damage to the Author's or the Author's institution's facilities, fraud, libel, defamation, research, equipment, experiments, property damage, personal injury, violations of institutional, laboratory, hospital, ethical, human and animal treatment, privacy or other rules, regulations, laws, procedures or guidelines, liabilities and other losses or damages related in any way to the submission of work to JoVE, making of videos by JoVE, or publication in *JoVE* or elsewhere by JoVE. The Author shall be responsible for, and shall hold JoVE harmless from, damages caused by lack of sterilization, lack of cleanliness or by contamination due to the making of a video by JoVE its employees, agents or independent contractors. All sterilization, cleanliness or decontamination procedures shall be solely the responsibility of the Author and shall be undertaken at the Author's
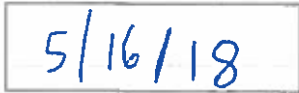
expense. All indemnifications provided herein shall include JoVE's attorney's fees and costs related to said losses or damages. Such indemnification and holding harmless shall include such losses or damages incurred by, or in connection with, acts or omissions of JoVE, its employees, agents or independent contractors.

12. Fees. To cover the cost incurred for publication, JoVE must receive payment before production and publication the Materials. Payment is due in 21 days of invoice. Should the Materials not be published due to an editorial or production decision, these funds will be returned to the Author. Withdrawal by the Author of any submitted Materials after final peer review approval will result in a US$1,200 fee to cover pre-production expenses incurred by JoVE. If payment is not received by the completion of filming, production and publication of the Materials will be suspended until payment is received.

13. Transfer, Governing Law. This Agreement may be assigned by JoVE and shall inure to the benefits of any of JoVE's successors and assignees. This Agreement shall be governed and construed by the internal laws of the Commonwealth of Massachusetts without giving effect to any conflict of law provision thereunder. This Agreement may be executed in counterparts, each of which shall be deemed an original, but all of which together shall be deemed to me one and the same agreement. A signed copy of this Agreement delivered by facsimile, e-mail or other means of electronic transmission shall be deemed to have the same legal effect as delivery of an original signed copy of this Agreement.

A signed copy of this document must be sent with all new submissions. Only one Agreement required per submission.

CORRESPONDING AUTHOR:

Name:	Mark R. Buckley
Department:	Department of Biomedical Engineering
Institution:	University of Rochester
Article Title:	Real-time Visualization and Analysis of Chondrocyte Death Due to Mechanical Loading in Fully Intact Murine Cartilage Explants
Signature:	*Mark R. Buckley* Date: 5/16/18

Please submit a signed and dated copy of this license by one of the following three methods:
1) Upload a scanned copy of the document as a pfd on the JoVE submission site;
2) Fax the document to +1.866.381.2236;
3) Mail the document to JoVE / Attn: JoVE Editorial / 1 Alewife Center #200 / Cambridge, MA 02139

For questions, please email submissions@jove.com or call +1.617.945.9051

3

612542.6

Responses to Reviewer Comments

We appreciate the insightful suggestions from the reviewers. In the following, we provide detailed responses to every comment. The manuscript was revised accordingly, and the changes were tracked to facilitate review.

Reviewer #1

Manuscript Summary: The authors have written an interesting manuscript. They describe a novel method of assess chondrocyte viability in a native mouse knee. The model described has a detailed protocol to ensure readers could duplicate the dissection required for the model.

We thank the reviewer for these compliments.

The model appears to have restriction toward younger mice, and this may be a limitation. The authors provide only one method of assessing chondrocyte viability without other technique to confirm the observed data. Finally, the authors choose to load the posterior femoral condyles without a clear explanation why this anatomic location has been chosen.

Major Concerns

1) The authors provide no other means of assessing chondrocyte viability other than Live / Dead staining and confocal microscopy assessment. Why not use other methods of assess viability to validate the model? Why should the reader accept this limited validation of the model?

We thank the reviewer for this important comment and apologize for not addressing this issue in the original manuscript. In fact, we considered several different alternatives to live/dead staining to assess cell viability and validate our model. However, we determined that none of these methods is able to capture the key outcome parameter of interest in our testing platform: the spatial extent of *in situ* cell injury/death on the surface of articular cartilage due to mechanical loading.

For example, in one class of alternative cell viability assessment techniques, histological evaluation of *in situ* chondrocytes is required. With some of these methods, the total number of nuclei (as assessed through analysis of H&E- or DAPI-stained sections) are counted as a surrogate measure of cell loss. However, while this approach is useful for quantifying long-term cell loss in the context of tissue degeneration, it cannot differentiate between viable and non-viable cells in the immediate aftermath of an injury (before the nuclei are cleared from the tissue). Another histological cell viability assessment technique – the TUNEL assay – is not appropriate for validation of our methodology, as it is only able to identify cells that die through apoptosis (whereas we

anticipate that necrosis dominates immediate mechanically induced cell death). Finally, it is important to note that even if a suitable histological cell viability assessment technique were identified, capturing the spatial extent of cell injury on the articular surface (the key outcome parameter of interest in our testing platform) would require time-consuming serial sectioning of paraffin-embedded specimens[1].

In another class of alternative cell viability assessment techniques, cell suspensions are required[2-5]. However, since murine articular cartilage is very small in size (e.g., articular surface width on femoral condyle < 1.5 mm, thickness < 50 μm), isolating cells from this tissue – especially in a specific region of interest (i.e., surrounding the site of injury) – is highly challenging. Moreover, isolating chondrocytes requires shaving cartilage from a joint, and the act of shaving itself could lead to additional cell injury/death that could confound results. Finally, most cell suspension-based methods (except those that work through the same principle as propidium iodide, one of the stains used in our study) only detect live cells, and thus require comparison to a control group for quantification of cell death. However, since these techniques generally have large coefficients of variation (e.g., 9.72% for the MTT assay[6], corresponding to approximately 1000 cells for a suspension of 10,000 cells), they cannot detect the small numbers of injured/dead cells induced by some loading regimens that can be easily quantified by live/dead staining. For instance, according to our findings, statically applied loading magnitudes of 0.1 N, 0.5 N and 1 N induce injury/death of just 3, 107 and 197 articular chondrocytes, respectively.

To avoid the limitations of cell suspensions, we did attempt to perform an alternative viability assay designed for cell suspensions but applied to the cartilage-on-bone explants used in our testing platform. In particular, we attempted to develop a tissue-based Alamar Blue assay. Alamar Blue is a resazurin reduction assay in which enzymatic activity of a cell is measured as a proxy for viable cells. In particular, viable cells reduce non-fluorescent resazurin to fluorescent resorufin. We followed a staining protocol used for the assessment of isolated mammalian cell cytotoxicity[7]. Briefly, after application of injurious loading, the dissected specimens were incubated in 10% of Alamar Blue at 37 °C for 4 h and 17 h later followed by 2 h wash in HBSS (pH 7.4, 303 mOsm). The specimens were imaged under fluorescent illumination at 560 nm excitation and 590 nm emission wavelengths. We hoped to observe bright fluorescence in viable cells, since metabolically active cells increase fluorescence by reduction of resazurin to resorufin. Unfortunately, since resorufin is membrane permeable and can escape to the extracellular matrix, it was nearly impossible to distinguish metabolically active cells from the surrounding ECM and surrounding non-viable cells. In other words, the entire specimen exhibited strong fluorescence, inhibiting our ability to detect live cells.

Although we were unable to provide an alternative validation for our live/dead staining-based quantification of cell injury/death, we have performed additional experiments to more rigorously investigate and quantify the limitations of live/dead staining. Presumably, the primary weakness of permeability stains like PI and calcein AM lies in the potential detection of false PI-positive and false calcein-negative cells due to their mechanism of action. For example, consider calcein AM, a molecule that is membrane permeant and non-fluorescent until it is cleaved by intracellular esterases and becomes

membrane impermeant and fluorescent. The fluorescent form of this molecule (calcein) remains within the cell while the membrane is intact; hence, calcein-positive cells are considered to be viable. However, if the membrane is only temporarily permeabilized (i.e., damaged prior to repair/resealing), a viable cell could appear calcein-negative. Similarly, consider PI is a membrane-impermeant molecule that is only able to diffuse into the cell and bind DNA if the membrane is not intact. A PI-positive cell is considered to have a ruptured membrane and be dead. However, if the membrane is only temporarily permeabilized (i.e., damaged prior to repair/resealing), a viable cell could appear PI-positive.

To investigate whether these limitations could be affecting our findings, we have conducted a pilot study (n=5) in which we longitudinally analyzed injury of *in situ* chondrocytes on femoral condyles immediately and 3 h after mechanical tests (0.5 N statically applied over 5 min) with calcein AM re-staining applied 2.5 h after the injury. The time scale of membrane repair is approximately 5 min[8]; thus, we presume that 2.5-3 h provides sufficient time to quantify the number of false PI-positive and false calcein-negative cells (i.e., the number of cells whose membrane was permeabilized only temporarily prior to repair/resealing). We found that the area of injured cells recovered by only 5.25% (approximately 22 cells per specimen) over the course of 180 min following the mechanical trauma (Figure R1). It is worth noting that cells in which the plasma membrane appeared to be repaired became both PI and calcein positive, a finding that is consistent with the mechanism of action of both permeability dyes.

Despite the absence of an alternative validation of our live/dead staining-based quantification of cell injury/death, these additional experiments (which are now described in the Supplementary Material section of the manuscript) suggest that in our system, live/dead staining (i.e., the use of permeability dyes) provides a reasonably accurate indication of cell viability, overestimating true viability by just 5%. Nevertheless, we have decided to alter the title and text to reflect that live/dead staining is a direct measure of membrane integrity that is not always indicative of cell viability. In particular, we define PI-positive and calcein-negative cells as "injured", where injury (and not necessarily cell death) is defined as a (potentially temporary) loss of plasma membrane integrity due to mechanical trauma.

The title now reads as "Real-time Visualization and Analysis of Chondrocyte Injury Due to Mechanical Loading in Fully Intact Murine Cartilage Explants".
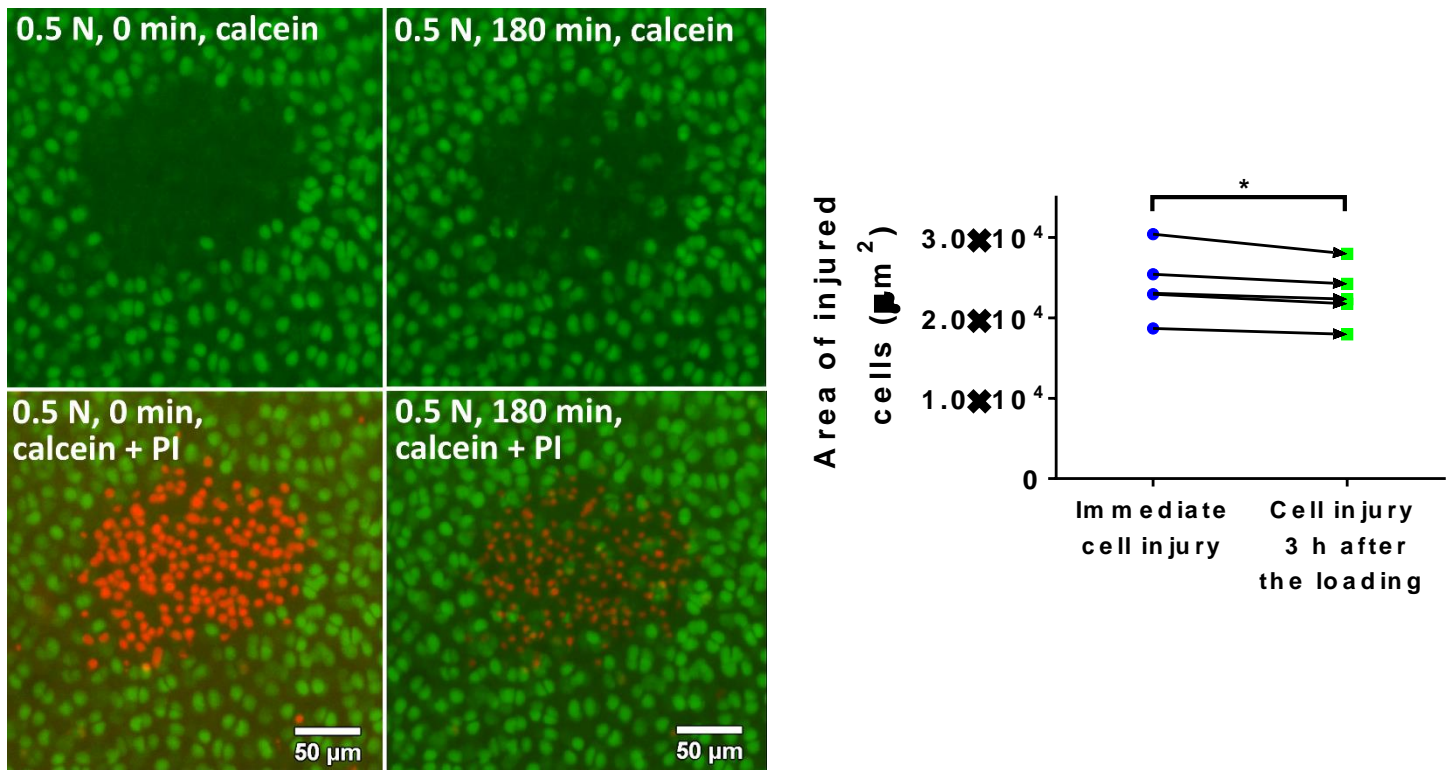
Figure R1 (Figure S2 in Supplemental Materials) (a) Representative micrographs of *in situ* articular chondrocytes on a medial femoral condyle obtained at 0 min (left) and at 180 min (right) after the application of mechanical loading (0.5 N static loading for 5 min). Green calcein fluorescence and the absence of red fluorescence indicate articular chondrocytes with intact plasma membranes; red PI fluorescence and the absence of green fluorescence indicate cells with compromised cell membrane integrity. The area/number of cells that gain calcein fluorescence within the 180 min time interval following mechanical trauma indicates the area/number of cells that exhibited membrane repair. Note that overall PI intensity has decreased over the 180 min time period, presumably due to photobleaching. (b) Area of injured cells (n=5) measured immediately (blue circles) and 180 min (green squares) after mechanical loading. Although the reduction in area of injured cells was significant, only approximately 5.25% of cells exhibited membrane repair. * denotes significance at α=0.05.

2) The authors describe a design of the impactor and confocal microscopy stage, but how they work together is unclear. The baseplate where loading occurs is a glass slide for microscopy - does the glass ever break with physiologically relevant loads?

We apologize for omitting these important details in our description of the mechanical testing platform. The impactor stage is built onto the stage plate of an inverted microscope (which may be either a standard epifluorescence microscope or a confocal laser scanning microscope). The glass slide (where the specimen is placed) sits on top of a stainless-steel plate screwed into the bottom of the base of the device. The center of the plate has a small pinhole (positioned below the location on the glass where specimen is placed) that serves as a viewing window for the inverted epifluorescence microscope. The pinhole/viewing window is sufficiently small that the glass resists bending and does not break under the loading conditions applied in this study (for both physiological and supraphysiological loading conditions).

We have added a paragraph describing these details to the supplementary material.

Minor Concerns:
3) The loads chosen - the authors report applied impact loads. Have the authors calculated the likely articular loads that occur with the model. Again, are these physiologically relevant?

We apologize for not clarifying the physiological relevance of the loads chosen for this study. For our studies using cartilage-on-femur explants, the load distribution on the medial and lateral condyles was measured previously[9]. In this study, we found that both the medial and lateral femoral condyles experience approximately 40% of the total applied load (with the contact point between the glass and femoral diaphysis taking up the remainder of the load). To our knowledge, the physiological loads on the cartilage of each compartment of the mouse knee have not been rigorously assessed. It has been shown that an axial load of approximated 9 N applied to the mouse tibia leads to bone strains similar to those induced during locomotion[10]. However, the axial load on the tibia is not equivalent to the load experienced by knee articular cartilage *in vivo* due to the complex geometry of the knee and the possible contributions of active muscles and passive surrounding tissues (e.g., the menisci). Nevertheless, we can determine the physiological relevance of each loading condition in our study by considering the strains induced in the tissue using our platform and comparing with physiological strains in the human knee reported in the literature (assuming physiological strains in articular cartilage are roughly conserved across species). For total applied loads of 0.1 N, we have previously measured peak compressive strains of 20.7% and 34% on the medial and lateral femoral condyles (data not shown). These strains are comparable to the reported strains of 39% observed in articular cartilage on the tibial plateau in human subjects after 30 min of standing[11]. Similarly, in unpublished studies, we have found that for a total applied load of 0.1 N on the murine humeral head, the peak strain is 31.6%

(data not shown). Previous studies have reported peak strains of 22% 9 min after push-up exercises[12]. During this waiting and imaging time (9 min), cartilage may have recovered its thickness, potentially resulting in an underestimate of peak strain during or immediately after exercise. Taken together, these finding suggest that the strains induced by 0.1N loading in our study lie within the upper limit of physiologically relevant strains. We consider higher magnitudes of static loading (0.5N and 1N) to be supraphysiological, since the peak strains surpass physiological levels and induce significant cell injury.

Unfortunately, confocal microscopy is not fast enough to capture tissue strains during impact experiments. However, we have performed additional studies to determine peak forces during these tests. Using a custom strain gauge apparatus, the peak impact forces were found to be higher than the statically applied forces. For example, a 1 mJ impact intensity induced a peak load of 8.3 N (data not shown). It is difficult to assess whether these forces lie within physiological limits in the absence of rigorous analyses of mouse joint mechanics during ambulation. We speculate that the impact-induced forces in this study are supraphysiological, given that substantial cell injury is induced in all experimental groups. However, it is important to note that impacts across a wide range of intensities (e.g., low intensity impact during ambulation and high intensity impacts during vehicle accidents) are clinically relevant.

The physiological relevance of the chosen loading conditions is now discussed in the Supplementary Material.

4) The authors discuss a limitation of the model is that mice used are very young. Older mice have "limited viability" with the harvest techniques. Why not load the joint axially or flip specimen 180 degrees to load anteriorly? Either of these techniques might be considered more realistic for day to day loading of a mouse knee. Will this solve this age problem? Many reports now suggest older joint behave very differently than young joints. This issue may be a limit in using the model more broadly.

We thank the reviewer for this useful feedback and helpful suggestion. It would be interesting to load the specimens from different angles; furthermore, doing so is feasible with our testing platform. This is now noted in the manuscript. However, in our representative data set, we decided to focus on a single location (the posterior femur) of high physiological relevance. Unlike the human, the mouse, as a quadruped, rarely stands on its hind limbs (such that its joint is loaded axially). During weight bearing, the mouse knee is usually flexed, resulting in contact between the tibia and posterior femur (Figure R2).
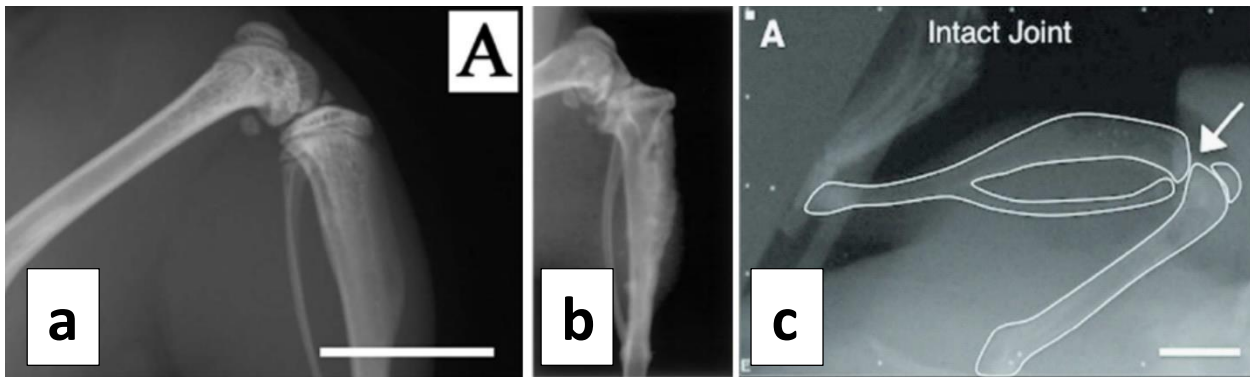
Figure R2 X-ray images of a murine knee joint adopted from (a) Yamawaki et al.[13], (b) McGary et al.[14], and (c) Adebayo et al.[10]. While x-ray images in (a) and (b) were taken to assess efficacy of a therapeutic drug, the x-ray image from (c) was used for analyses of knee kinematics recapitulating physiological loading of the tibia. White arrow indicates articular surface. All the images demonstrate that when the mouse knee is flexed, the primary point of contact between the tibia and the femur occurs at the posterior femoral condyles.

Regarding the applicability of our technique to older mice, through more careful dissections, we have recently overcome the limitation of reduced cell viability after dissecting aged mice (81 weeks old C57BL/6 mice). However, due to noticeable alterations in cell density in these mice, it is challenging though feasible (success rate = 40%) to assess load-induced cell injury in older femurs. In contrast, we did not notice alterations in cell density in articular cartilage on the humeral head of aged mice. Thus, we have been able to successfully apply our technique to the cartilage-on-humerus specimens from 81 week old (equivalent to the age of 65 years in a human) mice (Figure R3).

We adjusted the text in the limitation paragraph of the discussion to reflect these new observations and added these data to the Supplementary Material.
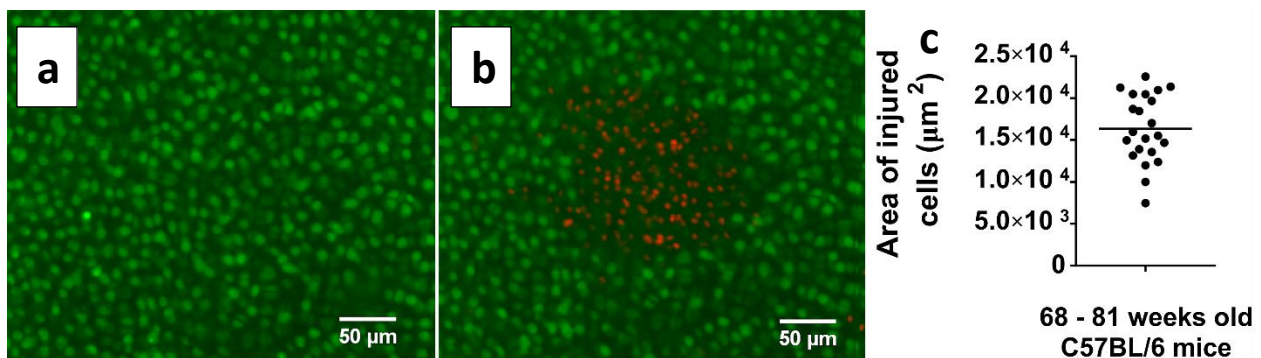

Figure R3 (Figure S3 in Supplementary Materials) Representative micrographs of *in situ* chondrocytes on the humeral head articular surface of an 81 week old male C57BL/6 mouse (a) at baseline and (b) after statically applied mechanical loading of 0.5 N for 5 min. Green calcein fluorescence and the absence of red fluorescence indicate

viable articular chondrocytes; red PI fluorescence and the absence of green fluorescence indicate injured/dead cells. (c) Area of injured cells, induced by 0.5 N statically applied for 5 min, quantified for specimens obtained from 68 – 81 weeks old C57BL/6 mice. Each data point represents a test on a different specimen and the mean value is indicated by horizontal bar.

Reviewer #2:
Manuscript Summary: In this manuscript, the authors presented a new method for studying controlled loading-induced cell death of intact murine femoral condyle and head joints. This is a very interesting method. In particular, this method offers a new method for understanding PTOA mechanisms in various genetic mice, and thus, has potentially transformative impact for studying PTOA. This paper is very well written, and detailed method steps are clearly presented. It can be published in the current form.

We thank the reviewer for these compliments.

Major Concerns:
No major concerns.

Minor Concerns:
There are some very minor points that may need clarification:
1) Page 5, line 138: "2.2.11) Remove the menisci…" Why would the menisci be a concern here? Menisci are attached on the tibia bone.

We thank the reviewer for this comment. We have removed this text from the manuscript, which now no longer refers to the meniscus. Instead, we emphasize removal of surrounding soft tissues (i.e., ligaments) from the femur to expose the articular surface.

2) For biological studies, is there any issue with potential contamination from bone marrow during the dissection and calcium imaging?

This is an interesting question. Although it is conceivable that contamination from bone marrow could occur, we have never observed evidence of isolated cells in our fluorescence images of the femoral and humeral articular surfaces. Thus, we do not believe that bone marrow cells have affected our representative findings. Nevertheless, we agree that it would be wise to take extra care to avoid this potential complication. Thus, the script was changed to read "after cutting the bone, wipe away any visible marrow on the outside of the bone to avoid possible contamination from bone marrow cells".

3) The representative data were obtained on 8-10 week old mice. What is the range of mouse age that this method is applicable to?

We thank the reviewer for this useful comment. As described in our response to Reviewer 1, through more careful dissections, we have recently overcome the limitation of reduced cell viability after dissecting aged mice (81 weeks old C57BL/6 mice). However, due to noticeable alterations in cell density in these mice, it is feasible (though more challenging) to assess load-induced cell injury in older femurs. In contrast, we did not notice alterations in cell density in articular cartilage on the humeral head of aged mice. Thus, we have been able to successfully apply our technique to the cartilage-on-humerus specimens from 81 week old (equivalent to the age of 65 years in a human) mice (Figure R3). Though we have not attempted these studies with mice older than 81 weeks or younger than 8 weeks, it is conceivable that there is an upper (and lower) age limit after which our technique no longer works. Nevertheless, we can safely state that our testing platform is useful for ages between 8 and 81 weeks. These details have been added to the manuscript and to the Supplementary Material (Figure R3).

Reviewer #3:
Manuscript Summary: Overall the manuscript is well written, easy to follow and of interest to others in the field

We thank the reviewer for these compliments.

Minor Concerns:

3.1.3 why centrifuge and vortex. Is vortexing not suffient? explanation here might be useful as it is not clear why this step should be treated in this way - other steps have explanations.

We apologize for not including the explanation of why we suggest both centrifugation and vortexing. When placing 1.25 μL of calcein AM stain into the microfuge tube containing 500 μL of HBSS, the dye may occasionally stick on the walls of the tube. Centrifugation ensures that all of the calcein AM dye mixes with the buffer. After centrifugation, we vortex to ensure proper mixing. The manuscript has been modified to clarify this rationale.

4.3 is there a need to do PI staining at this time to assess integity of tissue before mechanical testing? how do you know that the tissue is not damaged during dissection, or that the animal has some degree of cartilage damage? in the past I have found visibly normal tissue looks different once stained up and under miscroscope.

We thank the reviewer for this useful comment and observation. Our strategy to analyze the initial integrity of the tissue is through calcein AM straining, such that if there is initial damage, areas with obvious "gaps" in calcein-positive cells should be visible. That is, in every specimen, an initial fluorescence micrograph is acquired after calcein AM staining. The reviewer suggests an alternative method of analyzing the integrity of the tissue through PI staining before mechanical testing. To compare this approach to our own, we performed an experiment where a cartilage-on-femur specimen obtained from a 10 week old Balb/c female mouse was stained with both calcein AM and PI prior to mechanical testing (1N applied for 5 min) (Figure R4). At baseline, we observed a uniform distribution (without noticeable gaps) of calcein positive cells on the femoral condyles (Figure R4, left) and negligible numbers of randomly distributed PI-positive cells. In contrast, after mechanical testing, a clear and localized area of cells that lost calcein fluorescence and gained PI fluorescence was observed on both femoral condyles (Figure R4, right). This pilot study suggests that it is not necessary to stain cells with PI before an experiment. However, doing so provides a more rigorous confirmation that dissection-associated damage did not occur, and may be advisable – especially when the researcher is becoming acquainted with the dissection procedure. Hence, we have added PI staining prior to loading as an alternative approach in the protocol.
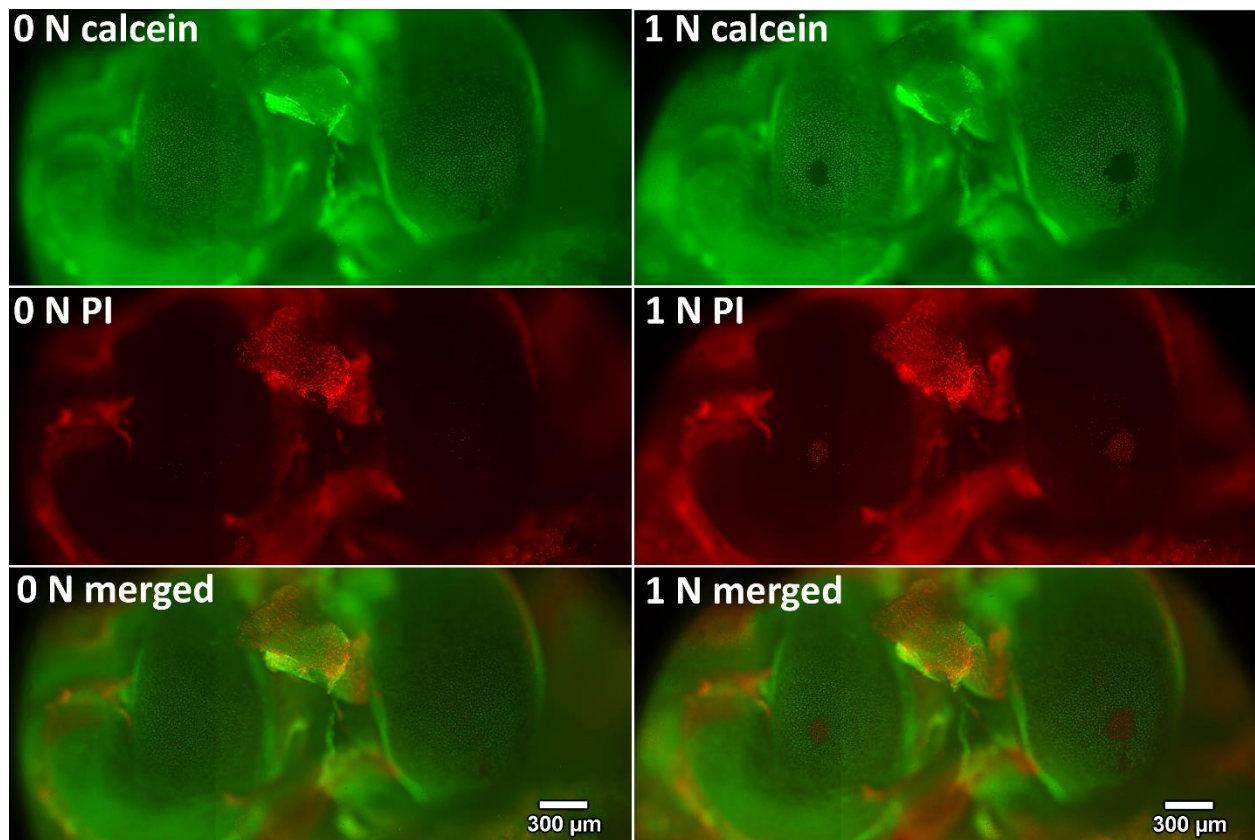

Figure R4 (Figure S1 in Supplementary Materials) Representative micrographs of *in situ* femoral condyle articular chondrocytes obtained at baseline (left) and after the

application of mechanical loading (1 N for 5 min, right). Green calcein fluorescence and the absence of red fluorescence indicate viable articular chondrocytes; red PI fluorescence and absence of green fluorescence indicate injured articular chondrocytes. These figures suggest that cell death patterns indicated by PI and calcein staining are consistent.

Line 299 Is the size of the injured area in comparison to the whole tissues physiologically relevant, or just the fact that the whole issue is the test environment being exposed in small areas to physiological loads - the text does not explictly state this in my opinion, and would benefit from this clarification - I am not sure this is replicating a physiological environment, but is likely to be more relevant than existing protocols.

We thank the reviewer for this useful feedback. As describe in our response to Reviewer 1, we can determine the physiological relevance of each loading condition in our study by considering the strains induced in the tissue using our platform and comparing with physiological strains in the human knee reported in the literature (assuming physiological strains in articular cartilage are roughly conserved across species). For total applied loads of 0.1 N, we have previously measured peak compressive strains of 20.7% and 34% on the medial and lateral femoral condyles (data not shown). These strains are comparable to the reported strains of 39% observed in articular cartilage on the tibial plateau in human subjects after 30 min of standing[11]. Similarly, in unpublished studies, we have found that for a total applied load of 0.1 N on the murine humeral head, the peak strain is 31.6% (data not shown). Previous studies have reported peak strains of 22% 9 min after push-up exercises[12]. During this waiting and imaging time (9 min), cartilage may have recovered its thickness, potentially resulting in an underestimate of peak strain during or immediately after exercise. Taken together, these finding suggest that the strains induced by 0.1N loading in our study lie within the upper limit of physiologically relevant strains. We consider higher magnitudes of static loading (0.5N and 1N) to be supraphysiological, since the peak strains surpass physiological levels and induce significant cell injury.

Unfortunately, confocal microscopy is not fast enough to capture tissue strains during impact experiments. However, we have performed additional studies to determine peak forces during these tests. Using a custom strain gauge apparatus, the peak impact forces were found to be higher than the statically applied forces. For example, a 1 mJ impact intensity induced a peak load of 8.3 N (data not shown). It is difficult to assess whether these forces lie within physiological limits in the absence of rigorous analyses of mouse joint mechanics during ambulation. We speculate that the impact-induced forces in this study are supraphysiological, given that substantial cell injury is induced in

all experimental groups. However, it is important to note that impacts across a wide range of intensities (e.g., low intensity impact during ambulation and high intensity impacts during vehicle accidents) are clinically relevant.

References

1   David, M. A. *et al.* Early, focal changes in cartilage cellularity and structure following surgically induced meniscal destabilization in the mouse. *Journal of Orthopaedic Research.* **35** (3), 537-547, doi:10.1002/jor.23443, (2017).

2   Prabst, K., Engelhardt, H., Ringgeler, S. & Hubner, H. Basic Colorimetric Proliferation Assays: MTT, WST, and Resazurin. *Cell Viability Assays: Methods and Protocols.* **1601** 1-17, doi:10.1007/978-1-4939-6960-9_1, (2017).

3   Riss, T. L. *et al.* in *Assay Guidance Manual*   eds G. S. Sittampalam *et al.*) (2004).

4   Repetto, G., del Peso, A. & Zurita, J. L. Neutral red uptake assay for the estimation of cell viability/cytotoxicity. *Nature Protocols.* **3** (7), 1125-1131, doi:10.1038/nprot.2008.75, (2008).

5   Smolina, N., Bruton, J., Kostareva, A. & Sejersen, T. Assaying Mitochondrial Respiration as an Indicator of Cellular Metabolism and Fitness. *Methods in Molecular Biology.* **1601** 79-87, doi:10.1007/978-1-4939-6960-9_7, (2017).

6   Petty, R. D., Sutherland, L. A., Hunter, E. M. & Cree, I. A. Comparison of MTT and ATP-based assays for the measurement of viable cell number. *Journal of Bioluminescence and Chemiluminescence.* **10** (1), 29-34, doi:10.1002/bio.1170100105, (1995).

7   O'Brien, J., Wilson, I., Orton, T. & Pognan, F. Investigation of the Alamar Blue (resazurin) fluorescent dye for the assessment of mammalian cell cytotoxicity. *European Journal of Biochemistry.* **267** (17), 5421-5426 (2000).

8   McNeil, P. L. & Kirchhausen, T. An emergency response team for membrane repair. *Nature Reviews Molecular Cell Biology.* **6** (6), 499-505, doi:10.1038/nrm1665, (2005).

9   Kotelsky, A., Woo, C. W., Delgadillo, L. F., Richards, M. S. & Buckley, M. R. An Alternative Method to Characterize the Quasi-Static, Nonlinear Material Properties of Murine Articular Cartilage. *Journal of Biomechanical Engineering.* **140** (1), doi:10.1115/1.4038147, (2018).

10   Adebayo, O. O. *et al.* Kinematics of meniscal- and ACL-transected mouse knees during controlled tibial compressive loading captured using roentgen stereophotogrammetry. *Journal of Orthopaedic Research.* **35** (2), 353-360, doi:10.1002/jor.23285, (2017).

11   Halonen, K. S. *et al.* Deformation of articular cartilage during static loading of a knee joint--experimental and finite element analysis. *Journal of Biomechanics.* **47** (10), 2467-2474, doi:10.1016/j.jbiomech.2014.04.013, (2014).

12   Zhang, H. *et al.* In Vivo Assessment of Exercise-Induced Glenohumeral Cartilage Strain. *Orthopaedic Journal of Sports Medicine.* **6** (7), 2325967118784518, doi:10.1177/2325967118784518, (2018).

13   Yamawaki, K. *et al.* The soluble form of BMPRIB is a novel therapeutic candidate for treating bone related disorders. *Scientific Reports.* **6** 18849, doi:10.1038/srep18849, (2016).

14   McGary, E. C. *et al.* Inhibition of platelet-derived growth factor-mediated proliferation of osteosarcoma cells by the novel tyrosine kinase inhibitor STI571. *Clinical Cancer Research.* **8** (11), 3584-3591 (2002).

Supplementary Material

1. Description of mechanical testing device

The impactor stage is built onto the stage plate of an inverted microscope, which may be either a standard epifluorescence microscope (used in this study) or a confocal laser scanning microscope. The mechanical testing device consists of a base with a glass slide (#1.5, 0.17 mm thick, 40 mm diameter) through which *in situ* articular chondrocytes can be visualized in real time. The glass slide is glued to the bottom of the elevated stainless-steel rim to serve as a cup for holding HBSS to hydrate the specimen. The specimen is placed onto the glass slide, which sits on top of a thin stainless-steel plate screwed into the bottom of the base (the stainless-steel rim) of the device. The center of the plate has a small pinhole (0.16" in diameter, positioned below the location on the glass where specimen is placed) that serves as a viewing window for the inverted epifluorescence microscope. The pinhole/viewing window is sufficiently small that the glass resists bending and does not break under the loading conditions applied in this study (for both physiological and supraphysiological loading conditions). The impactor guide block, which is vertically extended from the base, is a reamed bore through which a cylindrical weight can slide, thereby enabling application of controlled mechanical loads or impacts to the specimen. The loads can be applied either through a pulley system driven by computer-controlled linear actuator (for static or dynamic loading regimens) or by manually dropping a weight from different heights, resulting in impacts of different prescribed kinetic energies. (Figure 1 in the manuscript)

2. Physiological relevance of mechanical loading chosen for the study

The load distribution on the medial and lateral condyles of cartilage-on-femur explants was measured previously[1]. In this study, we found that both the medial and lateral femoral condyles experience approximately 40% of the total applied load (with the contact point between the glass and femoral diaphysis taking up the remainder of the load). To our knowledge, the physiological loads on the cartilage of each compartment of the mouse knee have not been rigorously assessed. It has been shown that an axial load of approximated 9 N applied to the mouse tibia leads to bone strains similar to those induced during locomotion[2]. However, the axial load on the tibia is not equivalent to the load experienced by knee articular cartilage *in vivo* due to the complex geometry of the knee and the possible contributions of active muscles and passive surrounding tissues (e.g., the menisci). Nevertheless, we can determine the physiological relevance of each loading condition in our study by considering the strains induced in the tissue using our platform and comparing with physiological strains in the human knee reported in the literature (assuming physiological strains in articular cartilage are roughly conserved across species). For total applied loads of 0.1 N, we have previously measured peak compressive strains of 20.7% and 34% on the medial and lateral femoral condyles (data not shown). These strains are comparable to the reported strains of 39% observed in articular cartilage on the tibial plateau in human subjects after 30 min of standing[3]. Similarly, in unpublished studies, we have found that for a total applied load of 0.1 N on the murine humeral head, the peak strain is 31.6% (data not shown). Previous studies have reported peak strains of 22% 9 min after push-up exercises[4]. During this waiting and imaging time (9 min), cartilage may have recovered its thickness, potentially resulting in an underestimate of peak strain during or immediately after exercise. Taken together, these finding suggest that the strains induced by 0.1N loading in our study lie within the upper limit of physiologically relevant strains. We consider higher magnitudes of static loading (0.5N and 1N) to be supraphysiological, since the peak strains surpass physiological levels and induce significant cell injury.

Unfortunately, confocal microscopy is not fast enough to capture tissue strains during impact experiments. However, additional studies have determined peak forces during these tests. Using a custom strain gauge apparatus, the peak impact forces were found to be higher than the statically applied forces. For example, a 1 mJ impact intensity induced a peak load of 8.3 N (data not shown). It is difficult to assess whether these forces lie within physiological limits in the absence of rigorous analyses of mouse joint mechanics during ambulation. We speculate that the impact-induced forces in this study are supraphysiological, given that substantial cell injury is induced in all experimental groups. However, it is important to note that impacts across a wide range of intensities (e.g., low intensity impact during ambulation and high intensity impacts during vehicle accidents) are clinically relevant.

3. **Alternative method of analyzing the integrity of the tissue through PI staining before mechanical testing**

The protocol described in the manuscript involves analysis of the initial integrity of the tissue (through calcein AM straining) to ensure that there is no initial damage (i.e., no areas with obvious "gaps" in calcein-positive cells should be visible). That is, in every specimen, an initial fluorescence micrograph is acquired after calcein AM staining. Alternatively, the integrity of the tissue can be analyzed through PI staining before mechanical testing. To compare this approach to the approach used in the manuscript, a cartilage-on-femur specimen obtained from a 10 week old Balb/c female mouse was stained with both calcein AM and PI prior to mechanical testing (1N applied for 5 min) (Figure S1). At baseline, a uniform distribution (without noticeable gaps) of calcein positive cells on the femoral condyles (Figure S1, left) and negligible numbers of randomly distributed PI-positive cells were observed. In contrast, after mechanical testing, a clear and localized area of cells that lost calcein fluorescence and gained PI fluorescence was observed on both femoral condyles (Figure S1, right). This pilot study suggests that it is not necessary to stain cells with PI before an experiment. However, doing so provides a more rigorous confirmation that dissection-associated damage did not occur, and may be advisable – especially when the researcher is becoming acquainted with the dissection procedure.
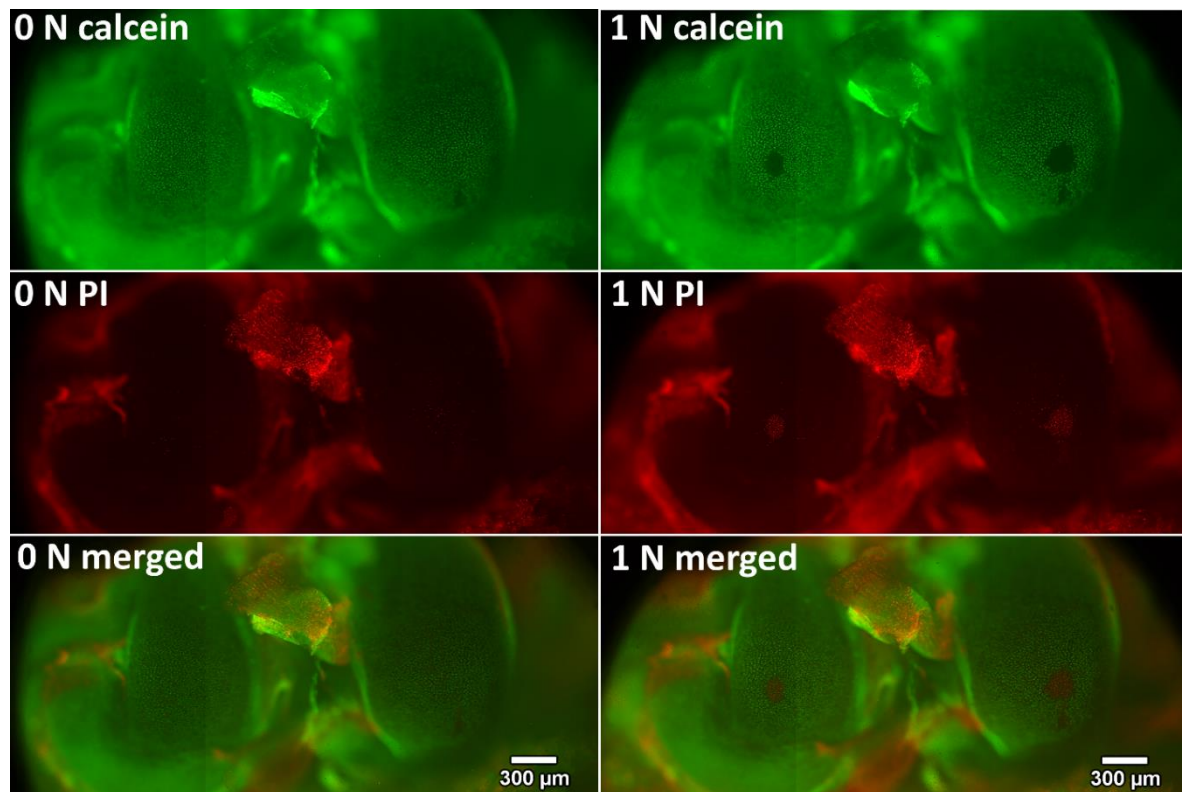

Figure S1 Representative micrographs of *in situ* femoral condyle articular chondrocytes obtained at baseline (left) and after the application of mechanical loading (1 N for 5 min, right). Green calcein fluorescence and the absence of red fluorescence indicate viable articular chondrocytes; red PI fluorescence and absence of green fluorescence indicate injured articular chondrocytes. These figures suggest that cell death patterns indicated by PI and calcein staining are consistent.

4. Limitations of live/dead staining as a measure of cell death

The primary weakness of permeability stains like PI and calcein AM lies in the potential detection of false PI-positive and false calcein-negative cells due to their mechanism of action. For example, consider calcein AM, a molecule that is membrane permeant and non-fluorescent until it is cleaved by intracellular esterases and becomes membrane impermeant and fluorescent. The fluorescent form of this molecule (calcein) remains within the cell while the membrane is intact; hence, calcein-positive cells are considered to be viable. However, if the membrane is only temporarily permeabilized (i.e., damaged prior to repair/resealing), a viable cell could appear calcein-negative. Similarly, consider PI is a membrane-impermeant molecule that is only able to diffuse into the cell and bind DNA if the membrane is not intact. A PI-positive cell is considered to have a ruptured membrane and be dead. However, if the membrane is only temporarily permeabilized (i.e., damaged prior to repair/resealing), a viable cell could appear PI-positive.

To confirm death of *in situ* articular chondrocytes due to mechanical loading, we have conducted a pilot study (n=5) in which we longitudinally analyzed injury of *in situ* chondrocytes on femoral condyles immediately and 3 h after mechanical tests (0.5 N statically applied over 5 min) with calcein AM re-staining applied 2.5 h after the injury. The time scale of membrane repair is approximately 5 min[5]; thus, we presume that 2.5-3 h provides sufficient time to quantify the number of false PI-positive and false calcein-negative cells (i.e., the number of cells whose membrane was permeabilized only temporarily prior to repair/resealing). We found that the area of injured cells recovered by only 5.25% (approximately 22 cells per specimen) over the course of 180 min following the mechanical trauma (Figure S2). It is worth noting that cells in which the plasma membrane appeared to be repaired became both PI and calcein positive, a finding that is consistent with the mechanism of action of both permeability dyes.

This experiment suggests that in our system, live/dead staining (i.e., the use of permeability dyes) provides a reasonably accurate indication of cell viability, overestimating true viability by just 5%.
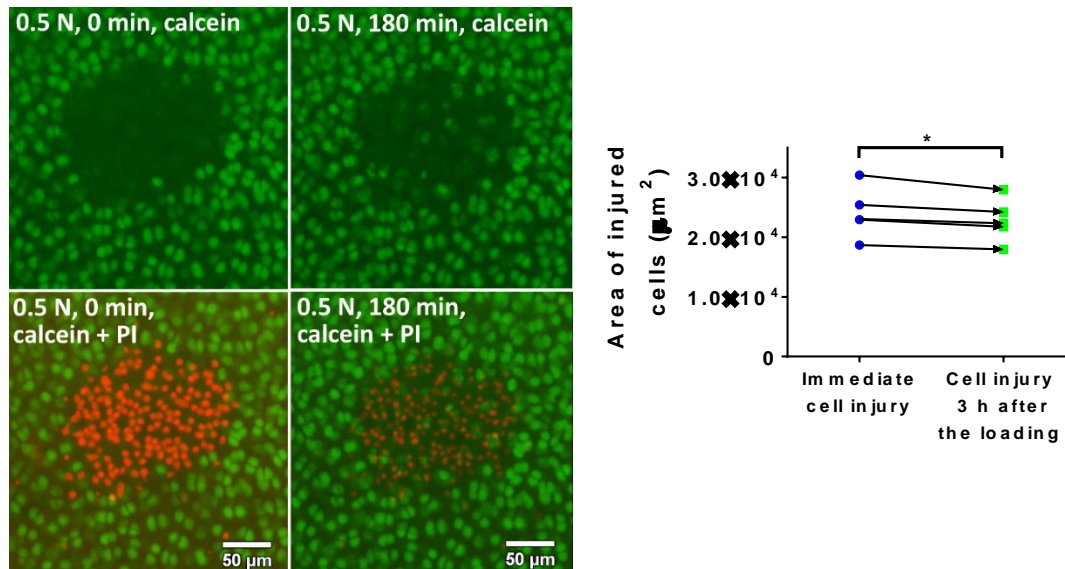

Figure S2 (a) Representative micrographs of *in situ* articular chondrocytes on a medial femoral condyle obtained at 0 min (left) and at 180 min (right) after the application of mechanical loading (0.5 N static loading for 5 min). Green calcein fluorescence and the absence of red fluorescence indicate articular chondrocytes with intact plasma membranes; red PI fluorescence and the absence of green fluorescence

indicate cells with compromised cell membrane integrity. The area/number of cells that gain calcein fluorescence within the 180 min time interval following mechanical trauma indicates the area/number of cells that exhibited membrane repair. Note that overall PI intensity has decreased over the 180 min time period, presumably due to photobleaching. (b) Area of injured cells (n=5) measured immediately (blue circles) and 180 min (green squares) after mechanical loading. Although the reduction in area of injured cells was significant, only approximately 5.25% of cells exhibited membrane repair. * denotes significance at α=0.05.

5. Use of the method in older mice

An additional set of experiments was performed to assess whether the method could be used in older mice. Cartilage-on-humerus explants of female and male C57BL/6 mice between 61 and 81 weeks old were tested using the protocol described in the manuscript. No additional difficulties were noted in performing these tests. However, attempted tests using cartilage-on-femur explants from these same mice yielded a success rate of just 40% (data not shown).
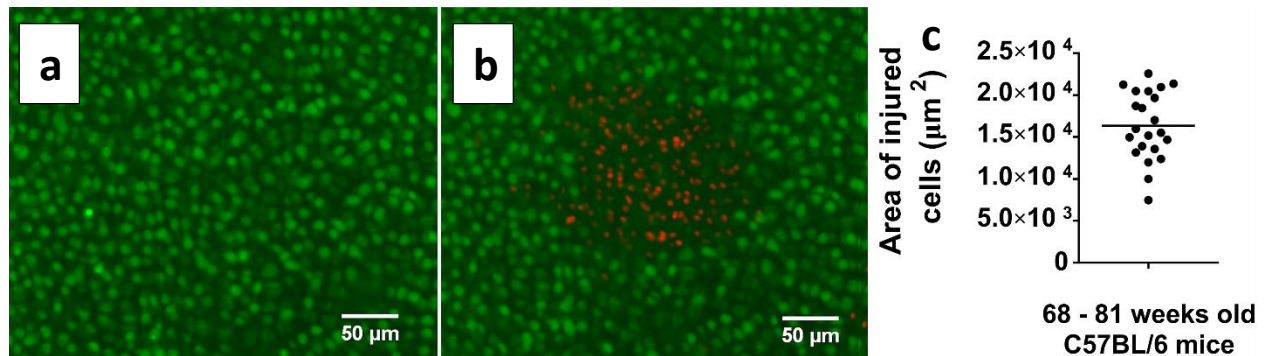

Figure S3 Representative micrographs of *in situ* chondrocytes on the humeral head articular surface of an 81 week old male C57BL/6 mouse (a) at baseline and (b) after statically applied mechanical loading of 0.5 N for 5 min. Green calcein fluorescence and the absence of red fluorescence indicate viable articular chondrocytes; red PI fluorescence and the absence of green fluorescence indicate injured/dead cells. (c) Area of injured cells, induced by 0.5 N statically applied for 5 min, quantified for specimens obtained from 68 – 81 weeks old C57BL/6 mice. Each data point represents a test on a different specimen and the mean value is indicated by horizontal bar.

References

1   Kotelsky, A., Woo, C. W., Delgadillo, L. F., Richards, M. S. & Buckley, M. R. An Alternative Method to Characterize the Quasi-Static, Nonlinear Material Properties of Murine Articular Cartilage. *Journal of Biomechanical Engineering.* **140** (1), doi:10.1115/1.4038147, (2018).

2   Adebayo, O. O. *et al.* Kinematics of meniscal- and ACL-transected mouse knees during controlled tibial compressive loading captured using roentgen stereophotogrammetry. *Journal of Orthopaedic Research.* **35** (2), 353-360, doi:10.1002/jor.23285, (2017).

3   Halonen, K. S. *et al.* Deformation of articular cartilage during static loading of a knee joint-- experimental and finite element analysis. *Journal of Biomechanics.* **47** (10), 2467-2474, doi:10.1016/j.jbiomech.2014.04.013, (2014).

4   Zhang, H. *et al.* In Vivo Assessment of Exercise-Induced Glenohumeral Cartilage Strain. *Orthopaedic Journal of Sports Medicine.* **6** (7), 2325967118784518, doi:10.1177/2325967118784518, (2018).

5   McNeil, P. L. & Kirchhausen, T. An emergency response team for membrane repair. *Nature Reviews Molecular Cell Biology.* **6** (6), 499-505, doi:10.1038/nrm1665, (2005).